This document was prepared in conjunction with work accomplished under Contract No. DE-AC09-96SR18500 with the U. S. Department of Energy.

DISCLAIMER

WSRC-TR-2005-00042
Revision 0

Dissolution of FB-Line Residues Containing Beryllium Metal

Tracy S. Rudisill and Mark L. Crowder

February 2005

Westinghouse Savannah River Company
Aiken, SC 29808

Prepared for the U. S. Department of Energy under Contract DE-AC09-96SR18500 (mod. 68)

This page was intentionally left blank.

Table of Contents

List of Tables

List of Figures

List of Appendices

Dissolution of FB-Line Residues Containing Beryllium Metal

Tracy S. Rudisill and Mark L. Crowder

Westinghouse Savannah River Company
Aiken, SC 29808

Summary

Scrap materials containing plutonium (Pu) metal are currently being transferred from the FB-Line vault to HB-Line for dissolution and subsequent disposition through the H-Canyon facility. Some of the items scheduled for dissolution contain both Pu and beryllium (Be) metal as a composite material. The Pu and Be metals were physically separated to minimize the amount of Be associated with the Pu; however, the dissolution flowsheet was required to dissolve small amounts of Be combined with the Pu metal using a dissolving solution containing nitric acid (HNO_3) and potassium fluoride (KF). Since the dissolution of Pu metal in HNO_3/fluoride (F^-) solutions is well understood, the primary focus of the experimental program was the dissolution of Be metal.

Initially, small-scale experiments were used to measure the dissolution rate of Be metal foils using conditions effective for the dissolution of Pu metal. The experiments demonstrated that the dissolution rate was nearly independent of the HNO_3 concentration over the limited range of investigation and only a moderate to weak function of the F^- concentration. The effect of temperature was more pronounced, significantly increasing the dissolution rate between 40 and 105°C. The offgas from three Be metal foil dissolutions was collected and characterized. The production of hydrogen (H_2) was found to be sensitive to the HNO_3 concentration, decreasing by a factor of approximately two when the HNO_3 was increased from 4 to 8 M. This result is consistent with the dissolution mechanism shifting away from a typical metal/acid reaction toward increased production of nitrogen oxides by nitrate (NO_3^-) oxidation.

Samples of contaminated Be previously separated from a Pu/Be composite material were subsequently dissolved in a 4 M HNO_3 solution containing 0.1-0.2 M KF targeting 70 and 80°C. Complete dissolution of the metal samples was achieved in 75-100 min. The heat produced by the Be dissolution and the insulating capacity of the heating mantle was sufficient to increase the solution temperature 10-20°C above the target values. Multiple gas samples collected during these experiments showed that the maximum H_2 generation rate occurred at temperatures below 70-80°C. At the lower temperatures, the dissolution of the Be by a metal/acid dissolution mechanism was apparently maximized. As the temperature increased above this range, the dissolution proceeded to a greater extent by NO_3^- oxidation resulting in the generation of brown nitrogen dioxide (NO_2) gas.

A Pu metal dissolution experiment was also performed using a 4 M HNO_3/0.1 M KF solution at 80°C to demonstrate flowsheet conditions developed for the dissolution of Be metal. As the dissolution progressed, the rate of dissolution slowed. The decrease in rate was attributed to the

complexation of F^- by the dissolved Pu. The F^- became unavailable to catalyze the dissolution of plutonium oxide (PuO_2) formed on the surface of the metal which inhibited the dissolution rate. Complete solubilization of the Pu was not achieved. Approximately 10% of the original material was recovered following the dissolution of a PuO_2-containing residue. Offgas analysis performed following the metal dissolution showed the presence of 2.6 vol% H_2 and a small amount of N_2O.

Based on the results of the Be and Pu metal dissolutions, the use of a 4M HNO_3 solution containing 0.15-0.2 M KF is recommended for the dissolution of approximately 500 g of Pu metal containing a minor amount of Be in an HB-Line dissolver batch. A dissolution temperature of 70-80°C should produce initial dissolution rates for the Pu and Be metal which are nominally the same. As the Pu metal dissolves, the Pu dissolution rate may slow due to the reduction in the free F^- by complexation with Pu and formation of PuO_2 on the metal surface. For this reason, an 8-10 h dissolution time is recommended which maximizes the dissolution temperature during the final 4-6 h to digest any PuO_2. Controls must also be in place to address the generation of H_2 which could be as high as 75 vol% of the offgas generated by the Be metal during the early stages of the dissolution.

Introduction

Scrap materials containing Pu metal are currently being transferred from the FB-Line vaults to HB-Line for dissolution and subsequent disposition through the H-Canyon facility. The materials are dissolved in Phase I of HB-Line and transferred to H-Canyon for interim storage until the final disposition path is defined. Some of the materials scheduled for disposition in the near future contain both Pu and Be metal. These composite materials will be dissolved in HB-Line using solutions containing HNO_3 and KF. No data are currently available for the simultaneous dissolution of both materials using this kind of flowsheet. However, available data for the dissolution of pure Be and Pu in HNO_3-based flowsheets are summarized below.

Be Metal Dissolution

Beryllium metal dissolves very slowly in HNO_3 solutions. The dissolution rate in 10 and 70 wt% solutions was measured by Darwin et al.[1] The data are summarized in Table 1.

Table 1 Beryllium Metal Dissolution in HNO_3 Solutions

HNO_3 Concentration (wt%)	(M)	Temperature	Test Duration (h)	Mass Loss (mg/cm^2-h)
10	1.67	Room	60	2.8
10	1.67	Boiling	0.1	8
72	15.6	Room	60	0.03
72	15.6	Boiling	0.1	20

The slow rate of dissolution in concentrated HNO_3 at room temperature can be attributed to passivation of the Be surface due to the formation of a beryllium oxide coating. Dilute acid (at room temperature) has a slight, but measurable, rate of attack. The dissolution rate in boiling HNO_3 is much higher, but would still be an inefficient and time consuming means to dissolve Be metal. The data in Table 1 were generated by exposing small samples of massive extruded Be to reagent grade HNO_3. The reaction in boiling acid was described as far from violent; however, the authors speculated that the use of powdered Be could generate more energetic conditions. This behavior would likely be true, since the rate of dissolution of solids is generally proportional to the available surface area.

In a more detailed study, Hardy et al. [2] performed a series of dissolutions using both Be metal sheet and tubes. In most of the experiments, the rate of dissolution during the first 0.5 to 1 h was usually greater than the final constant value; however, this result was thought to be due to a surface effect associated with the sheet and tube fabrication methods. The final constant dissolution rates at 97°C for Be metal sheet and tubes as a function of the HNO_3 concentration are plotted on Figure 1. The rates for the tube are generally lower than for the sheet, but follow the same trends, being approximately independent of the HNO_3 concentration from 6 to 14 M. Beryllium dissolution rates were also reported to increase markedly with temperature.

Beryllium metal is soluble to a greater extent in other solvents. The relative dissolution rates for common acids are compared below.

$$HF > H_2SO_4 \approx HCl > HNO_3$$

The metal dissolves rapidly in 3 M sulfuric acid (H_2SO_4) and 5 M ammonium fluoride (NH_4F).[1] Beryllium like aluminum (Al), dissolves in strong bases, forming the beryllate (BeO_2^{2-}) ion (equation 1).[1,3]

$$Be + 2\ KOH \rightarrow K_2BeO_2 + H_2 \quad (1)$$

Metallic Be is also rapidly dissolved by ammonium bifluoride (NH_4HF_2). The reaction (equation 2) has been used as the basis for scrap recovery on an industrial scale.[1]

$$2\ NH_4HF_2 + Be \rightarrow (NH_4)_2BeF_4 + H_2 \quad (2)$$

The rate of Be dissolution in HNO_3 solutions containing F^- has also been evaluated. Hardy et al. [2] performed a series of experiments in 14 M HNO_3 at 50°C with hydrofluoric acid (HF) concentrations that varied between 0 and 0.5 M. Above 0.1 M HF, the reaction became very vigorous and caused the temperature to rise almost to the boiling point. The rate of dissolution in solutions containing greater than 0.01 M HF was initially fast but became constant at approximately 0.04 mg/cm^2-min. The initial dissolution rates were much higher, increasing linearly from nominally 0.2 to 1.5 mg/cm^2-min as the HF concentration was increased from 0.05 to 0.25 M. A reduction in the dissolution rate did not occur until enough Be dissolved to produce a Be:HF molar ratio which exceeded 3:1.

A dissolution flowsheet for ^{238}Pu scrap containing Be and brass was developed at the SRS.[4] Dissolution rate data for cylinders of Be-containing $^{238}PuO_2$ scrap as a function of HNO_3 and HF concentrations are reproduced on Figure 2. The dissolution rates were measured under reflux conditions. The rates increase with both the addition of F^- and as the HNO_3 concentration increases in the same general manner as the data presented on Figure 1.

Pu Metal Dissolution

The dissolution of Pu metal using a HNO_3/KF flowsheet was investigated at both the Rocky Flats Plant and the SRS. Miner et al. performed a series of experiments in which unalloyed (alpha phase) Pu metal was dissolved in solutions containing 1-5 M HNO_3 and 0.01-0.13 M HF at 26-69°C.[5] The maximum rate of dissolution occurred at approximately 3 M HNO_3 in combination with an HF concentration of 0.13 M (the highest investigated) at any temperature between 26 and 69°C. Additional dissolution experiments with alpha and delta-stabilized metal were performed by Holcomb at the SRS.[6-7] The focus of these experiments was the effect of the Al^{3+} concentration on the dissolution rate. The experiments verified the optimal flowsheet recommended by Miner et al. and demonstrated that the dissolution rate was sensitive to the presence of Al^{3+} and other elements which complex F^-. Complexation of F^- decreases its activity in solution and effectiveness as a catalyst for the dissolution of PuO_2. The dissolution of both alpha and delta-stabilized metal in HNO_3 requires a small amount of free F^- to inhibit the

formation of a PuO_2 layer on the surface of the metal due to oxidation by HNO_3. Generally, the rate of dissolution increases with the F^- concentration and is only constrained by plutonium tetrafluoride (PuF_4) precipitation. The HNO_3 concentration must also remain dilute to reduce the surface oxidation rate. This requirement is even more important for delta-stabilized metal. Karraker reported that the surface of delta-stabilized Pu metal was much more reactive toward nitrate (NO_3^-) oxidation than that of alpha phase metal.[8]

Based on the work of Miner et al. and Holcomb, the use of a dissolving solution containing nominally 3 M HNO_3-0.1 M F^- was considered optimal for the dissolution of both alpha and delta-stabilized Pu metal at temperatures ranging from 25-90°C. Under these conditions, dissolution rates in the range of 5-10 mg/cm^2-min would be expected.[5-7]

Hydrogen Generation

The dissolution of both Be and Pu metals result in the generation of offgases containing H_2. During the development of the dissolution flowsheet for ^{238}Pu scrap containing Be and brass, [4] offgases containing 12 vol% H_2 were produced by boiling 10 M HNO_3 containing ≤ 0.01 M F^-. The balance of the offgas was reported as nitric oxide (NO). In those experiments, the production of H_2 was attributed almost entirely to the dissolution of Be; gases evolved during the dissolution of brass contained less than 0.01 vol% H_2. In that study, 0.69 mole of offgas was produced for every mole of Be dissolved. The H_2:NO ratio was also reported to be independent of the HNO_3 concentration. In a subsequent study, Thompson [9] analyzed the gases produced when Be metal was dissolved in 1-15 M HNO_3 solutions containing 0.1 M F^-. At each HNO_3 concentration, the evolved gas contained 75 vol% H_2 and 25 vol% NO. The increase in the H_2 concentration shows that the additional F^- shifts the Be dissolution mechanism from HNO_3 oxidation to a typical metal-acid reaction (equation 3).

$$Be + 2\ HNO_3 \rightarrow Be(NO_3)_2 + H_2 \qquad (3)$$

In those experiments, 0.88 mole of offgas was produced for every mole of Be dissolved.

Only limited data are available concerning the concentration of H_2 and other gases produced during the dissolution of Pu metal using solutions containing HNO_3 and F^-. Miner et al. reported that gas samples withdrawn from just above the surface of the dissolving solution at various times during dissolution always contained ≤ 0.3 vol% H_2. The gas produced in the highest concentration was nitrous oxide (N_2O). The gases were analyzed by gas chromatography. The minimum detection limit for H_2 was 0.05 vol%.

Experimental Objectives

The Pu/Be composite materials to be dissolved in the HB-Line Phase I facility were physically separated to minimize the amount of Be associated with the Pu; however, a flowsheet must still be designed to dissolve small amounts of Be combined with the Pu metal in the dissolver charge. Since the dissolution of Pu metal in HNO_3/F^- solutions is well understood, the primary focus of this experimental program was the dissolution of Be metal. A series of small-scale experiments was performed in which dissolution rates of Be metal foils were measured using dissolving

conditions effective for the dissolution of Pu metal. As part of these experiments, the composition and quantity of offgas produced were measured during several demonstrations of aggressive dissolving conditions. In subsequent experiments, optimal flowsheet conditions were demonstrated for the dissolution of samples of contaminated Be metal removed from a composite material and a sample of scrap FB-Line Pu metal. The composition and quantity of offgas generated during the demonstration experiments were also measured. The experimental methods used to perform these experiments and a discussion of the results and observations are presented in the following sections.

Experimental

Dissolution Rate of Be Metal Foil

A series of small-scale experiments was completed in which dissolution rates of Be metal were determined. The dissolution rates were measured using 25 mm x 25 mm x 0.5 mm Be metal foils containing nominally 0.6 g of metal; the Be assay was 99.5%. The dissolutions were performed in a 500 mL three-neck flask using a porous glass basket attached to the center stopper to hold and allow access to the foil. A water-cooled condenser was attached to the flask to reduce the evaporation of the dissolving solution. The dissolving solution was heated and stirred using a heating mantle equipped with a magnetic stirrer. The temperature of the dissolving solution was monitored using an alcohol-filled thermometer. The calibration of the alcohol thermometer was established using a calibrated mercury-filled thermometer. Photographs of the dissolving system and glass basket are shown on Figure 3.

Dissolutions were performed using solutions containing 3-8 M HNO_3/0.0135-0.2 M KF at 40°C to boiling (105°C). The experiments were performed by initially preheating the dissolving solution to the desired temperature, inserting the Be foil into the flask using the glass basket, and periodically removing the foil to measure the mass and surface area (i.e., length, width, and thickness of the foil). Dissolution rates were calculated as the rate of change of the mass to surface area ratio as a function of time.

Offgas Characterization from Be Metal Foil Dissolution

In subsequent experiments, the volume and composition of the offgas generated during the dissolution of Be metal foils were measured. The experiments were performed in the same manner as the experiments used to measure the dissolution rates. To sample and collect the offgas, the exit from the condenser on the dissolver was connected with ¼ inch plastic tubing to an approximate 25 mL sample bulb and 1 L Tedlar bag. The sample bulb was fabricated with glass stopcocks on the ends to provide a means to isolate the sample. Quick disconnects (which seal upon disconnection) were used to attach and remove the sample bulbs and Tedlar bags from the plastic tubing.

To perform an experiment, the Be metal foil was loaded into the glass basket and suspended in the flask above the level of the dissolving solution. The solution was preheated to the desired temperature and air was removed from the system by purging with argon for nominally 10 min. The argon supply was attached to the dissolving vessel using a glass stopper fabricated with a quick disconnect. Following the argon purge, an evacuated Tedlar bag was connected to the sample bulb exit. The dissolution was initiated by lowering the glass basket containing the Be foil into the dissolving solution. The offgas was collected until the Be foil was completely dissolved. The volume of gas collected during a dissolution was determined by the difference in the amount of water displaced by the empty (evacuated) and filled bag. Gas analyses were performed by gas chromatography.

Three dissolution experiments were performed in which the volume and composition of the offgas were measured. Dissolving solutions containing 4 M HNO_3/0.1 M KF, 4 M HNO_3/0.2 M KF, and 8M HNO_3/0.1 M KF were used during dissolution experiments. A dissolution temperature of 80°C was targeted for the experiments; although, the heat of reaction from the metal dissolution raised the temperature to 90-100°C during each experiment.

Contaminated Be Metal Dissolution

A series of dissolution experiments was performed using nominally 2.5 g samples of contaminated Be metal received from the FB-Line Facility. The metal samples were physically separated from a composite material to be dissolved in HB-Line. The objectives of the experiments were to compare the dissolution of the contaminated material to the dissolution of the Be metal foils and to characterize the offgas produced during the dissolution. A 1 L, three-neck flask was used for the dissolutions; other laboratory equipment was essentially the same as used for the Be metal foil dissolutions. During the experiments, 2-5 gas samples were taken to characterize the offgas throughout the dissolution process. Air was initially removed from the dissolving vessel and plastic tubing by purging with nitrogen (N_2). The sample bulbs were also purged with N_2 for nominally 10 min prior to use. Tedlar bags used to collect the offgas were evacuated by vacuum pump. The volume of gas collected in each bag was determined as the difference in the amount of water displaced by the filled and evacuated bags. Gas analyses were performed by gas chromatography.

The contaminated Be metal dissolutions were performed using a 4 M HNO_3 solution containing 0.1-0.2 M KF. Dissolution temperatures of 70 and 80°C were targeted for the experiments; although, the heat of reaction from the metal dissolutions raised the temperatures above these values. A 650 mL aliquot of the dissolving solution was used in each experiment which would simulate the dissolution of 50-60 g of Be in 15 L of solution in an HB-Line dissolver. This amount of Be is approximately 10% of the normal Pu charge and would be expected to represent a typical amount of Be associated with the Pu/Be composite material. For experiments performed using 0.1 M KF, this volume of solution also results in an approximate 4:1 mole ratio of Be to F^- (upon complete dissolution) which was the highest ratio investigated during the Be dissolution rate measurements. When the Be metal was added to the dissolver, the glass basket was suspended above the solution during the N_2 purge. Once the purging was complete, the glass basket was lowered into the solution, the heating mantle and stirrer were energized, and the gas sample bulb and Tedlar bag were connected to the plastic tubing attached to the offgas condenser. When the first and subsequent gas samples were taken, the sample bulb and Tedlar bag were disconnected from the condenser exit and a new bulb and bag were connected. Therefore, calculation of the offgas composition for a sample period must take into account the mixing of the offgas with gases already present in the dissolving vessel, condenser, and connection tubing.

Pu Metal Dissolution

To demonstrate the dissolution of Pu metal using a HNO_3/KF flowsheet, an experiment was performed in which 23 g of scrap metal from FB-Line were added to a 650 mL aliquot of a 4 M HNO_3/0.1 M KF solution. A dissolution temperature of 80°C was selected as the target value.

These conditions were expected to generate a dissolution rate of nominally 10 mg/cm^2-min based on previous studies at the Rocky Flats Plant.[5] The solid to liquid ratio in this experiment was equivalent to dissolving 500 g of Pu in the 15 L working volume of an HB-Line dissolver. The experiment was performed in the same equipment as used for the contaminated Be metal dissolution. During the experiment, two gas samples were taken to characterize the offgas from the dissolution. The mass of Pu dissolved during each sample time was determined by removing the Pu metal and measuring the mass before and after the collection period. Air was purged from the dissolving vessel and plastic tubing using N_2 prior to sampling. The sample bulbs were purged with argon prior to use. The Tedlar bags used to collect the offgas were evacuated by vacuum pump. The volume of gas collected in each bag was determined by water displacement and analysis was performed by gas chromatography.

This page was intentionally left blank.

Results and Discussion

Dissolution Rate of Be Metal Foil

The experimental data used to calculate the dissolution rate of the Be metal foils as a function of the conditions are given in Appendix A. Dissolution rates were calculated as the rate of change of the mass to surface area ratio of the Be metal as a function of the dissolving time and by convention are reported as negative values. Plots of the data and linear regressions for each dissolution experiment are also presented in Appendix A. A summary of the conditions and measured rates for each Be metal foil dissolution is given in Table 2.

Table 2 Be Metal Foil Dissolution Rates

Experiment No.	HNO_3 (M)	KF (M)	Temperature (°C)	Rate (mg/cm^2-min)
Be-1	3	0.1	40	-0.47
Be-2	4	0.1	40	-0.52
Be-3	4	0.15	40	-0.67
Be-4	4	0.1	60	-1.1
Be-5	4	0.1	80	-2.5
Be-6	4	0.1	105	-7.7
Be-7	8	0.1	40	-0.41
Be-8	4	0.2	40	-0.71
Be-9	4	0.2	105	-9.2
Be-12	4	0.0135	40	-0.21

Inspection of the data in Table 2 show that the Be metal dissolution rate was nearly independent of the HNO_3 concentration in the range of investigation and only a moderate to weak function of the F^- concentration. However, the effect of temperature was significantly more pronounced, increasing the rate of dissolution by a factor of approximately 15 between 40 and 105°C. These observations are generally consistent with the work by Hardy et al. [2] and the work performed at the SRS [4] in which the Be metal dissolution rate was not a strong function of either the HNO_3 or F^- concentrations, but increased markedly with temperature.

Temperature Dependence of Rate Constant

If the mechanism for the dissolution of Be metal in HNO_3/F^- solutions was known, an expression for the reaction rate in terms of the HNO_3 and F^- concentrations and a temperature dependent rate constant could be written. However, if one assumes the rate of dissolution is independent of the HNO_3 concentration over the range of investigation, the reaction becomes pseudo zero order for a constant F^- concentration and is only a function of temperature (equation 4).

$$- \text{Rate} = k(T) \tag{4}$$

The temperature dependence of the rate constant can be calculated from the data in Table 2 (at 0.1 M KF) by assuming the dependence is represented by Arrhenius' Law:

$$k(T) = k_0 e^{-\frac{E}{RT}} \quad (5)$$

where E is the activation energy of the reaction and k_0 is the frequency factor. Equations 4 and 5 illustrate that a plot of log(-Rate) versus 1/T should be linear with a slope of -E/ln(10)R and a y-intercept of $\log(k_0)/\ln(10)$. The 0.1 M KF data from Table 2 are plotted on Figure 4 and generally show a linear relationship between the two variables. For comparison, the two data points at 0.2 M KF are also shown on the figure. The calculated activation energy and frequency factor for each KF concentration are given in Table 3.

Table 3 Parameters for Arrhenius Temperature Dependence

KF (M)	E (KJ/mole)	K_0
0.1	41.6	3.89×10^6
0.2	39.3	2.55×10^6

An activation energy of nominally 40 KJ/mole would be described as moderately temperature sensitive (i.e., the reactants must be heated to achieve a significant dissolution rate).[10] Predictably, the activation energy for the data at 0.2 M KF is lower than the activation energy at 0.1 M due to the increased KF concentration.

Offgas Characterization from Be Metal Foil Dissolution

Three experiments were performed in which the volume and composition of the offgas produced from the dissolution of a Be metal foil were measured. The raw data from the gas analyses were adjusted to account for dilution from gas in the freeboard region of the dissolution vessel, condenser, plastic tubing, and sample bulb. The analyzed concentrations and the methodology used to calculate the adjusted concentrations are summarized in Appendix B. The adjusted concentrations and a summary of the conditions for each dissolution are given in Table 4. The dissolution temperature for each experiment was 90-100°C.

Table 4 Characterization of Offgas from Be Metal Foil Dissolutions

Expt. No.	HNO_3 (M)	KF (M)	Offgas:Be (mole:mole)	H_2 (mol%)	NO (mol%)	N_2O (mol%)
Be-13	4	0.1	0.31	42	28	5.1
Be-14	8	0.1	0.31	26	45	20
Be-15	4	0.2	0.30	46	28	4.2

The data in Table 4 show that the production of H_2 was sensitive to the HNO_3 concentration. When the HNO_3 was increased from 4 to 8 M, the concentration of H_2 in the offgas was reduced by a factor of approximately two. This result is consistent with the dissolution mechanism

shifting away from a typical metal/acid reaction (equation 3) toward increased production of nitrogen oxides (by equations 6-8). The presence of NO_2 in the offgas was identified based on the light brown color of the collected gas; however the gas chromatograph configuration was not capable of this analysis.

$$Be + 2\ HNO_3 \rightarrow Be(NO_3)_2 + H_2 \quad (3)$$

$$Be + 4\ HNO_3 \rightarrow Be(NO_3)_2 + 2\ NO_2 + 2\ H_2O \quad (6)$$

$$3\ Be + 8\ HNO_3 \rightarrow 3\ Be(NO_3)_2 + 2\ NO + 4\ H_2O \quad (7)$$

$$4\ Be + 10\ HNO_3 \rightarrow 4\ Be(NO_3)_2 + N_2O + 5\ H_2O \quad (8)$$

The ratio of offgas produced to the amount of Be dissolved during each experiment was essentially constant at 0.31 mole/mole. This ratio is considerably less than the values (0.69 and 0.88 mole/mole) measured during previous work at the SRS.[4,9] The lower value could be attributed to the adsorption of nitrogen oxides by the dissolving solution and oxidation back to HNO_3 and potentially to changes in the dissolution path (i.e., reaction) as a function of temperature.

Heat of Reaction for Be Metal Dissolution

The target temperature for performing the Be metal foil dissolutions used for offgas characterization was 80°C. The solution was preheated to this value prior to starting each dissolution; however, during the experiments, the temperature of the solution increased to 90-100°C. The heat of reaction for equations 3 and 6-8 was calculated from standard heats of formation,[11] and are given in Table 5.

Table 5 Heat of Reactions for Be Metal Dissolution

Equation No.	Heat of Reaction (KJ/mole Be Dissolved)
3	-452.9
6	-611.9
7	-658.5
8	-703.2

The heat of reaction for each dissolution path is exothermic; therefore, it is not surprising to see a temperature rise in the dissolving solution when the reaction rate becomes sufficiently rapid. The magnitude of the temperature rise is dependent upon the heat transfer characteristics of the dissolution system. The heating mantle used in the experiments was well insulated and cooled very slowly.

Contaminated Be Metal Dissolution

The time required to completely dissolve the contaminated Be metal samples is summarized in Table 6.

Table 6 Time to Dissolve Contaminated Be Metal Samples

Expt. No.	Be Metal Mass (g)	Solution HNO_3 (M)	Solution KF (M)	Target Temperature (°C)	Maximum Temperature (°C)	Dissolution Time (min)
Be-17	2.3043	4	0.1	80	101	75
Be-18	2.2973	4	0.1	70	77	150
Be-19	2.7097	4	0.1	70	91	100
Be-20	2.5308	4	0.2	70	87	100

The dissolution times given in Table 6 are approximate; the times were based on visual observations that no metal remained in the dissolving vessel. In each experiment, the dissolution proceeded slowly at first based on the observed gas collection rate. When the temperature reached 60-70°C, gas generation increased and the appearance of the gas collected in the Tedlar bag became browner in color. The brown gas indicated changes in the dissolution path at the higher temperatures which resulted in the production of more NO_2 (equation 6). In experiments Be-18, Be-19, and Be-20, an effort was made to minimize the temperature increase above 70°C by turning the heating mantle off (at approximately 65°C) prior to reaching the target temperature. However, in each experiment the heat produced by the Be dissolution and the insulating capacity of the heating mantle was sufficient to increase the temperature 10-20°C above the target values. The temperature profiles of the dissolving solution are plotted on Figure 5. It should be noted that the temperature profiles are specific to the laboratory-scale equipment used in the experiment and would not be the same for the HB-Line dissolver due to different insulating and heat transfer properties.

In general, the contaminated Be samples and the Be metal foils dissolved in a consistent manner; although, the volume of offgas generated by the sample dissolved in experiment Be-18 was considerably less than the volume generated in the other experiments (see following discussion). The dissolving solution was filtered (using medium porosity paper, > 2.5 μm particle retention) following each experiment; however, very few residual solids were collected. Samples of the solution from experiments Be-17 and Be-18 were analyzed for ^{238}Pu and $^{239/240}Pu$ by thenolytrifluoroacetone (TTA) extraction/alpha pulse height analysis (APHA) and trace metal constituents by Inductively Coupled Plasma Emission Spectroscopy (ICP-ES). The ratios of Pu to Be in the samples were 0.003 and 0.008 g Pu/g Be, respectively. The elemental analysis for the two solutions and the estimated mass of each element, based on the final volume of dissolving solution, are shown in Table 7.

Table 7 Elemental Analysis for Be Metal Dissolving Solutions

Element	Experiment No. Be-17		Experiment No. Be-18	
	Concentration (mg/L)	Mass (mg)	Concentration (mg/L)	Mass (mg)
Ag	0.118	0.0792	<0.100	N/A
Al	12.9	8.66	18.6	12.4
B	19.7	13.2	15.6	10.4
Ba	0.350	0.235	0.245	0.163
Be	2880	1930	3780	2520
Ca	2.51	1.68	2.04	1.36
Cd	<0.084	N/A	<0.210	N/A
Ce	<0.488	N/A	<1.22	N/A
Cr	6.70	4.50	1.99	1.33
Cu	0.333	0.223	0.790	0.527
Fe	4.51	3.03	3.81	2.54
Gd	0.130	0.087	<0.130	N/A
K	3810	2560	3460	2310
La	0.686	0.460	0.568	0.379
Li	<0.084	N/A	<0.210	N/A
Mg	0.834	0.560	0.416	0.277
Mn	0.329	0.221	0.213	0.142
Mo	12.2	8.19	14.5	9.67
Na	49.4	33.1	28.5	19.0
Ni	1.07	0.718	<0.290	N/A
P	<3.00	N/A	<7.51	N/A
Pb	<2.12	N/A	<5.29	N/A
S	<0.888	N/A	<2.22	N/A
Sb	29.5	19.8	41.9	27.9
Si	160	107	137	91.4
Sn	13.5	9.06	10.3	6.87
Sr	2.13	1.43	1.87	1.25
Ti	0.714	0.479	0.615	0.410
U	0.909	0.610	<1.55	N/A
V	0.170	0.114	N/M	N/M
Zn	1.06	0.711	1.14	0.760
Zr	0.302	0.203	0.260	0.173

N/A – Not Applicable
N/M – Not Measured

The analyses of the solutions used for the dissolution of the two samples show that the Be metal was very pure. Impurities other than potassium (K, from the KF used in the dissolving solution) which have the highest concentrations include silicon (Si), sodium (Na), and antimony (Sb). The Si is likely from the corrosion of the dissolving vessel during the dissolution and the Na could be present as an impurity in the KF. It is unclear whether the Sb was present as an impurity in the

Be metal or the concentration was biased high due to interferences between elements during the ICP-ES analyses.

During the contaminated Be dissolutions, multiple gas samples were collected to characterize the offgas. The raw data from the gas analyses were adjusted in the same manner as the analyses from the dissolution of the Be metal foils to account for dilution from gas in the dissolution vessel, condenser, plastic tubing, and sample bulb. The analyzed concentrations and calculation of the adjusted concentrations are summarized in Appendix B. The adjusted concentrations, sample time interval, temperature range, and volume of offgas collected are shown in Table 8.

Table 8 Characterization of Offgas from Contaminated Be Metal Dissolutions

Expt./Sample No.	Time Interval (min)	Temperature Range (°C)	Offgas Collected (mL)	Adjusted H_2 (vol%)	Adjusted N_2O (vol%)
Be-17/1	0-30	23-79	233	31	BDL
Be-17/2	30-36	79-96	259	NR	2.7
Be-17/3	36-41	96-100	608	3.2	NR
Be-17/4	41-53	100-101	737	9.7	0.46
Be-17/5	53-75	101-97	18	17	10.6
Be-18/1	0-70	24-71	411	76	0.35
Be-18/2	70-150	71-77-68	31	NR	BDL
Be-19/1	0-60	24-75	428	19	0.11
Be-19-2	60-70	75-83	342	8.8	4.6
Be-19/3	70-75	83-87	193	NR	NR
Be-19/4	75-100	87-91-82	487	1.2	0.21
Be-20/1	0-60	24-71	373	55	BDL
Be-20/2	60-73	71-80	265	NR	1.7
Be-20/3	73-82	80-85	598	NR	0.67
Be-20/4	82-87	85-87	504	3.9	1.3
Be-20/5	87-100	87-82	213	1.3	NR

NR – not reported
BDL – below detection limit

The data in Table 8 show that the maximum H_2 generation rate occurred at temperatures below 70-80°C. At lower temperatures, the dissolution of the Be by a metal/acid dissolution mechanism (equation 3) was apparently maximized. As the temperature increased above this range, the dissolution proceeded to a greater extent by NO_3^- oxidation (equations 6-8). This assertion is supported by the color of the offgas observed in the Tedlar bags. The offgas collected during the initial sample interval generally had less color than the offgas collected during the remainder of the experiments. A number of adjusted concentrations in Table 8 were not reported due to a low bias in the measured concentration which in combination with the volume of offgas collected resulted in the calculation of a negative concentration.

The amount of offgas collected as a function of the amount of Be dissolved during each experiment is summarized in Table 9.

Table 9 Ratio of Offgas Produced to Amount of Be Dissolved

Experiment No.	Offgas:Be Ratio (mole/mole)
Be-17	0.30
Be-18	0.07
Be-19	0.20
Be-20	0.28

The offgas:Be ratios for experiments Be-17 and Be-20 are consistent with the 0.31 mole/mole collected during the dissolution of the Be metal foils. The ratio for experiment Be-19 was biased low due to a leak from the dissolution system when the quick disconnect on one of the Tedlar bags was not properly seated and flow was obstructed. The low value obtained for experiment Be-18 cannot be completely explained. The Be metal used in this experiment was different in appearance from the other three samples. The sample was thicker and the edges were rougher in appearance where the material was broken. The elemental analysis of the dissolving solutions for experiments Be-17 and Be-18 (see Table 7) do not show a significant difference; therefore, the difference in the offgas generation rates cannot be attributed to differences in composition. Hardy et al. reported differences in the dissolution (rate) behavior of Be metal for materials which were fabricated using different methods. [2] Therefore, it is possible that the fabrication history of the Be metal sample could have influenced its dissolution behavior resulting in the generation of less offgas. The Be metal samples used in experiments Be-17, Be-19, and Be-20 were similar in appearance and generally dissolved the same.

Pu Metal Dissolution

The conditions selected for the Pu metal dissolution were expected to generate a dissolution rate of nominally 10 mg/cm^2-min based on work performed at Rocky Flats.[5] At the beginning of the experiment, the dissolution rate was probably consistent with this value; however, as the dissolution progressed, the rate of dissolution slowed. The first 72% of the metal was dissolved/oxidized in approximately 5 h. The last 18% of the metal required 7.5 h for complete dissolution/oxidation. The steady decrease in the dissolution rate was attributed to the complexation of F^- by the dissolved Pu. The F^- became unavailable to catalyze the dissolution of PuO_2 which formed on the surface of the metal and inhibited the dissolution rate. A reduction in the final Pu concentration and/or an increase in the F^- concentration would improve the overall dissolution rate; however, precipitation of PuF_4 should be avoided.

Complete solubilization of the Pu was not achieved. Plutonium oxide solids generated during the dissolution were collected by filtration (using medium porosity paper, > 2.5 μm particle retention). No Pu metal was observed in the solids. The filter paper and solids were calcined at 600°C, ground, and dissolved in boiling 8 M HNO_3/0.1 M KF for 3 h. The resulting solution was then filtered upon cooling. Essentially all of the solid material dissolved. The filter paper collected a small amount of very fine white powder which was probably silica from corrosion of

the dissolution vessel. Samples of the solutions from the Pu metal and residue dissolutions were analyzed for ^{238}Pu and $^{239/240}Pu$ by TTA extraction/APHA and for ^{241}Pu and americium-241 (^{241}Am) by gamma pulse height analysis (GPHA). An elemental analysis was performed by ICP-ES. Results from these analyses are given in Appendix C.

The radiochemical analyses indicated that 90% of the Pu metal dissolved during the initial dissolution. As noted above, the decrease in the dissolution rate and formation of PuO_2 was probably due to a reduction in the free F^- concentration from complexation with Pu. An increase in the F^- concentration to 0.15-0.2 M is recommended to increase the dissolution rate and decrease the amount of PuO_2 which forms during dissolution. An increase of this magnitude would not be expected to cause the precipitation of PuF_4. The ICP-ES analysis shows that the Pu metal was relatively pure. The presence of the small amount of impurities would have essentially no influence on the dissolution characteristics of the metal.

During the analysis of the offgas samples from the Pu dissolution, one of the samples was contaminated with air. The H_2 concentration in the remaining offgas sample when adjusted for dilution (see Appendix B) was 2.6 vol%. A small amount (1.4 vol%) of N_2O was detected. The presence of NO_2 was also identified based on the light brown color of the collected offgas. The total volumes of gas collected during the two sample periods were 0.17 and 0.48 mole of offgas per mole of Pu dissolved.

Conclusions

A series of small-scale dissolutions was used to measure the dissolution rate of Be metal foils in (3-8 M) HNO_3 solutions containing (0.0135-0.2 M) KF at 40-105°C. The experiments demonstrated that the dissolution rate was nearly independent of the HNO_3 concentration over the range of investigation and only a moderate to weak function of the F^- concentration. The effect of temperature was more pronounced, increasing the dissolution rate by a factor of approximately 15 between 40 and 105°C. The temperature dependence of a pseudo zero order rate constant for 0.1 and 0.2 M F^- was calculated by assuming the rate was independent of the HNO_3 concentration and the temperature dependence was represented by Arrhenius' Law. The calculated activation energy of nominally 40 KJ/mole indicates the dissolution rate is moderately temperature sensitive (i.e., requiring the heating of reactants to achieve a significant dissolution rate).

In subsequent experiments, the offgas from three Be metal foil dissolutions was collected and analyzed to characterize the composition and volume of offgas. The production of H_2 was found to be sensitive to the HNO_3 concentration. When the HNO_3 was increased from 4 to 8 M, the concentration of H_2 in the offgas was reduced by a factor of approximately two. This result is consistent with the dissolution mechanism shifting away from a typical metal/acid reaction toward increased production of nitrogen oxides by NO_3^- oxidation. The presence of NO_2 in the offgas could not be quantified, but was identified based on the light brown color of the collected gas. The ratio of offgas produced to the amount of Be dissolved during each experiment was essentially constant at 0.31 mole/mole.

Four samples of contaminated Be previously separated from a Pu/Be composite material were dissolved in a 4 M HNO_3 solution containing 0.1-0.2 M KF targeting dissolution temperatures of 70 and 80°C. Complete dissolution of the metal samples was achieved in 75-100 min. The dissolution of the metal proceeded slowly at first based on the observed gas collection rate. When the temperature reached 60-70°C, gas generation increased and the appearance of the collected gas became browner in color. The heat produced by the Be dissolution and the insulating capacity of the heating mantle was sufficient to increase the solution temperature 10-20°C above the target values. Multiple gas samples collected during each experiment showed that the maximum H_2 generation rate occurred at temperatures below 70-80°C. At the lower temperatures, the dissolution of the Be by a metal/acid dissolution mechanism was apparently maximized. As the temperature increased above this range, the dissolution proceeded to a greater extent by NO_3^- oxidation resulting in the generation of brown NO_2 gas. The offgas:Be ratios were generally consistent with the value obtained for the Be metal foils; although, one experiment produced a surprisingly low value which might be attributed to the fabrication history of the sample.

A Pu metal dissolution experiment was performed using a 4 M HNO_3/0.1 M KF solution at 80°C to demonstrate flowsheet conditions developed for the dissolution of Be metal. These conditions were expected to generate a Pu dissolution rate consistent with the rate observed for Be metal. At the beginning of the experiment, the rate was likely consistent with this value; however, as the dissolution progressed, the rate of dissolution slowed. The steady decrease in the dissolution rate was attributed to the complexation of F^- by the dissolved Pu. The F^- became unavailable to

catalyze the dissolution of PuO_2 formed on the surface of the metal which inhibited the dissolution rate. Complete solubilization of the Pu was not achieved. Plutonium oxide solids collected by filtration and calcined at 600°C easily dissolved in boiling 8 M HNO_3/0.1 M KF after 3 h. The analysis of solutions from dissolution of the metal and solids indicated that 90% of the Pu metal dissolved. An increase in the F^- concentration to 0.15-0.2 M is recommended to increase the dissolution rate and decrease the amount of PuO_2 solids which form during dissolution. Offgas analysis performed following the metal dissolution showed the presence of 2.6 vol% H_2 and a small amount of N_2O. The presence of NO_2 was also identified based on the light brown color of the collected offgas. The total volume of gas collected during the sample period was 0.17 mole of offgas per mole of Pu dissolved.

Flowsheet Recommendations

The use of a 4 M HNO_3 solution containing 0.15-0.2 M KF is recommended for the dissolution of approximately 500 g of Pu metal containing minor amounts (≈ 50 g) of Be in the 15 L working volume of an HB-Line dissolver. A dissolution temperature of 70-80°C should produce initial dissolution rates for the Pu and Be metal which are nominally the same. As the Pu metal dissolves, the Pu dissolution rate may slow due to the reduction in the free F^- by complexation with Pu. The reduction in the free F^- will result in the formation of increased amounts of PuO_2 on the metal surface which inhibits metal dissolution. For this reason, an 8-10 h dissolution time is recommended to digest any PuO_2 solids; the temperature of the dissolving solution should be maximized during the final 4-6 h of the dissolution to facilitate the digestion of the solids.

The dissolution of both Pu and Be metal generate offgases containing H_2 which is a flammability concern. Dilution below 25% of the lower flammability limit is generally required. The H_2 concentration measured in the offgas during the dissolution of Pu metal was only 2.6 vol%; however, a H_2 concentration of 76 vol% was measured during the initial stages of one Be metal dissolution. The limited amount of Be associated with the Pu minimizes the flammability concern, but controls must still be in place to address the issue.

This page was intentionally left blank.

References

1. G. E. Darwin, and J. H. Buddery, *Metallurgy of the Rarer Metals – 7, Beryllium*, Academic Press Inc., New York, NY (1960).

2. C. J. Hardy and D. Scargill, *The Dissolution of Beryllium in Aqueous Mineral Acids and Ammonium Fluoride*, J. Chem. Soc. Part III, pp. 2658-2663 (1961).

3. F. A. Cotton and G. Wilkinson, *Advanced Inorganic Chemistry*, 5th Edition, John Wiley & Sons, New York, NY, p. 148 (1988).

4. *Technical Manual, Plutonium-238 Scrap Recovery, Building 221-H*, Report DPSTM-^{238}Pu-SCRAP, E. I. du Pont de Nemour & Co., Aiken, SC (1975).

5. F. J. Miner, J. H. Nairn, and J. W. Berry, *Dissolution of Plutonium in Dilute Nitric Acid*, I&EC Product Research and Development, **9**, pp. 402-405 (1969).

6. H. P. Holcomb, *Dissolving Alpha-Phase Plutonium Metal*, Report WSRC-RP-89-00616, Westinghouse Savannah River Company, Aiken, SC (1989).

7. H. P. Holcomb, *Laboratory-Scale Dissolution of Delta-Phase Plutonium Metal*, Report WSRC-TR-90-0101, Westinghouse Savannah River Company, Aiken, SC (1990).

8. D. G. Karraker, *Dissolution of Plutonium Metal in HNO_3-N_2H_4-KF*, Report DP-1666, E. I. du Pont de Nemours & Co., Aiken, SC (1983).

9. M. C. Thompson, *Hydrogen Production in the Dissolution of Beryllium*, Report DPST-76-282, E. I. du Pont de Nemour & Co., Aiken, SC (1976).

10. O. Levenspiel, *Chemical Reaction Engineering*, 2nd Edition, John Wiley & Sons, New York, NY, pages 28-29 (1972).

11. J. A. Dean, Editor, *Lange's Handbook of Chemistry*, 13th Ed., McGraw-Hill Book Company, New York, NY (1985).

This page was intentionally left blank.

Figure 1 Dissolution of Be Metal in HNO_3[2]

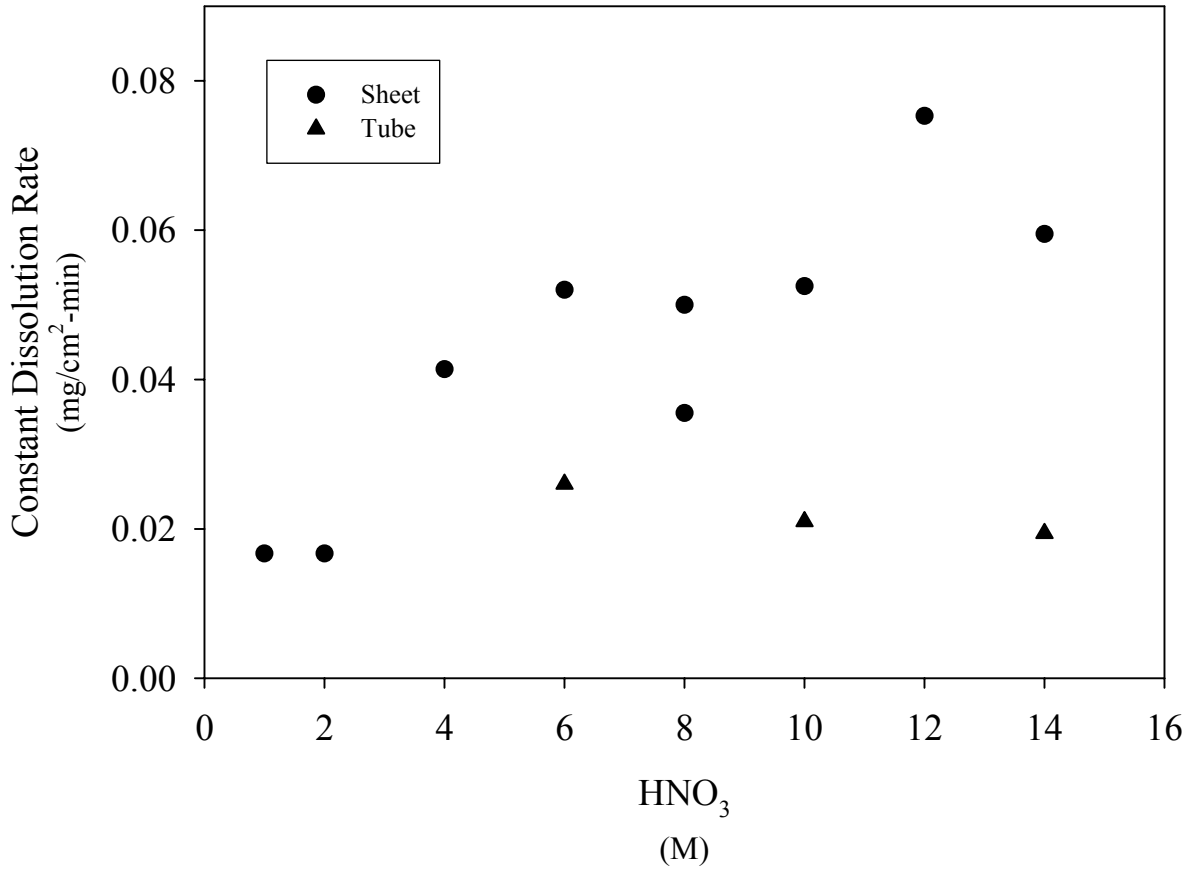

This page was intentionally left blank.

Figure 2 Dissolution Rate of Cylinders of Be-containing $^{238}PuO_2$ Scrap[4]

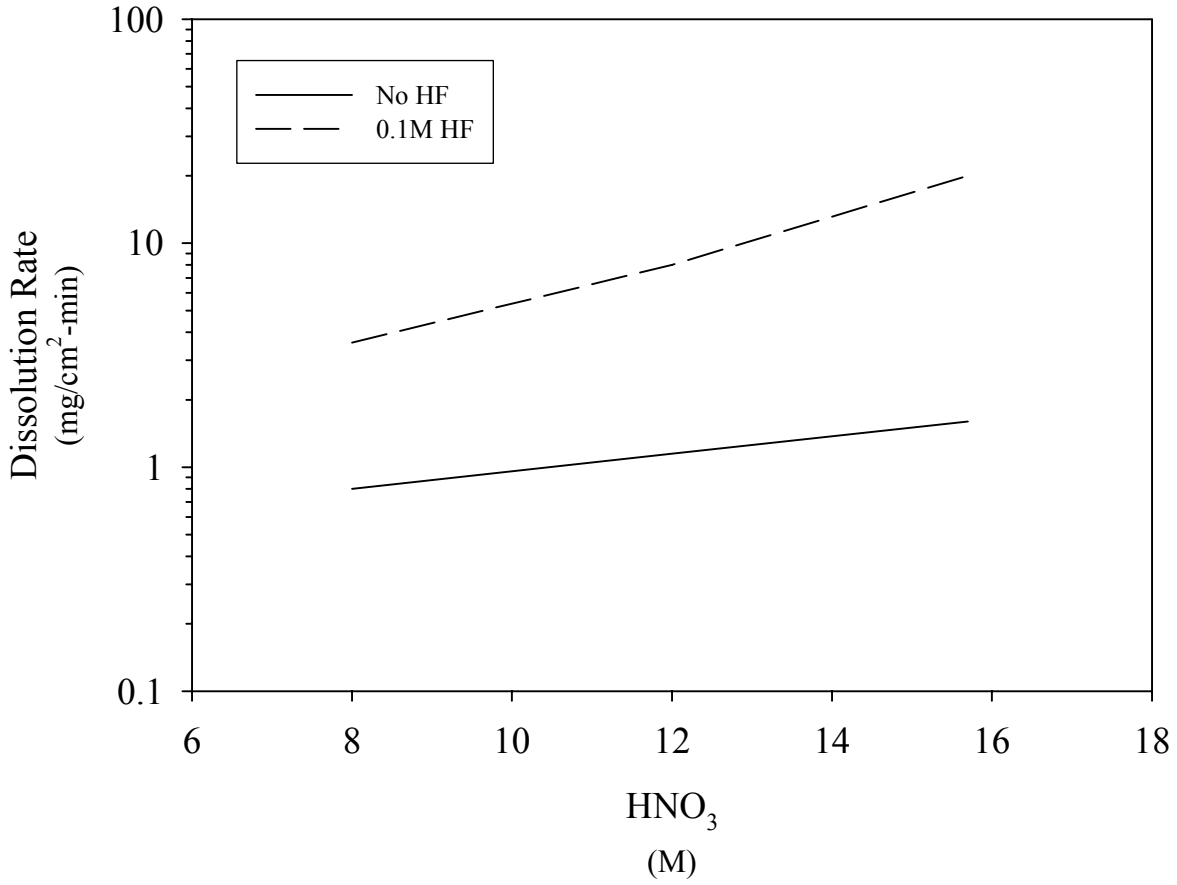

This page was intentionally left blank.

Figure 3 Be Metal Dissolution Equipment

Heating Mantle and Dissolution Vessel

Glass Dissolving Basket

This page was intentionally left blank.

Figure 4 Arrhenius Temperature Dependence of Dissolution Rate Constant

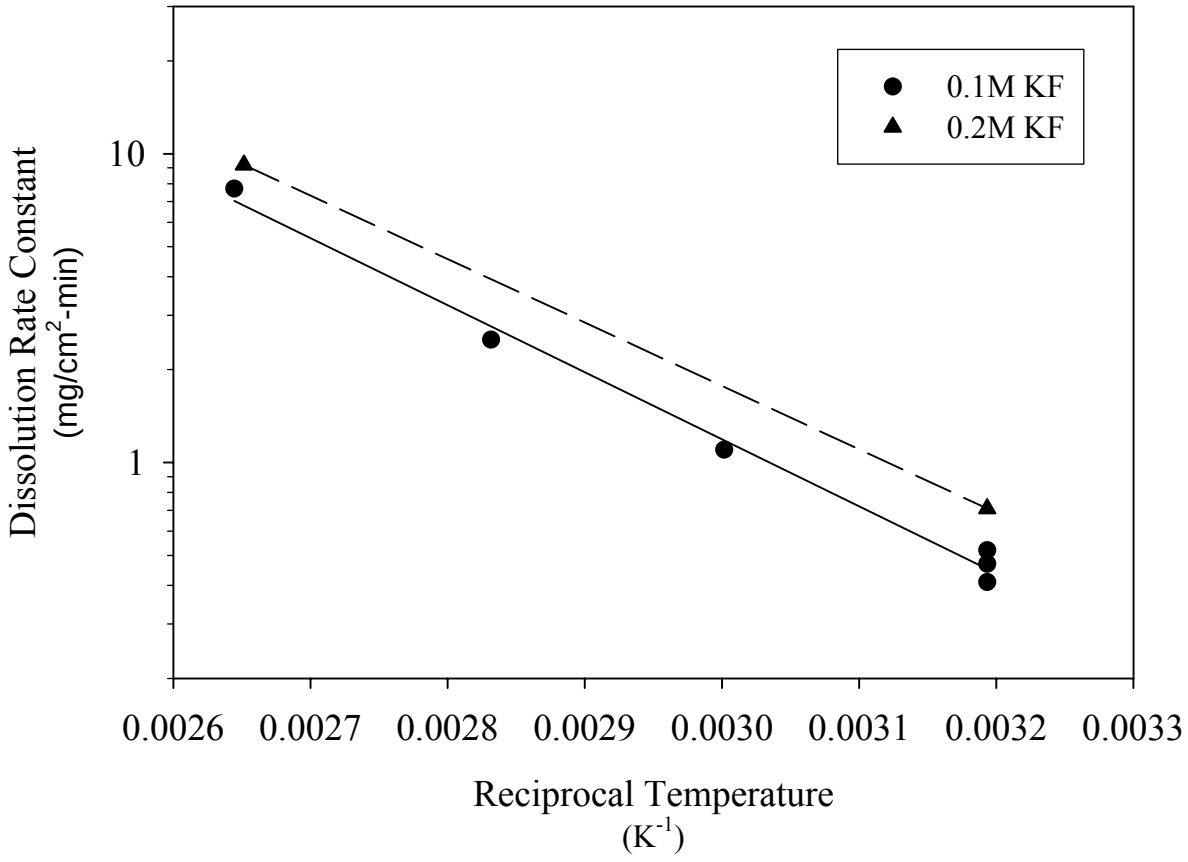

This page was intentionally left blank.

Figure 5 Temperature Profiles of Be Metal Dissolving Solutions

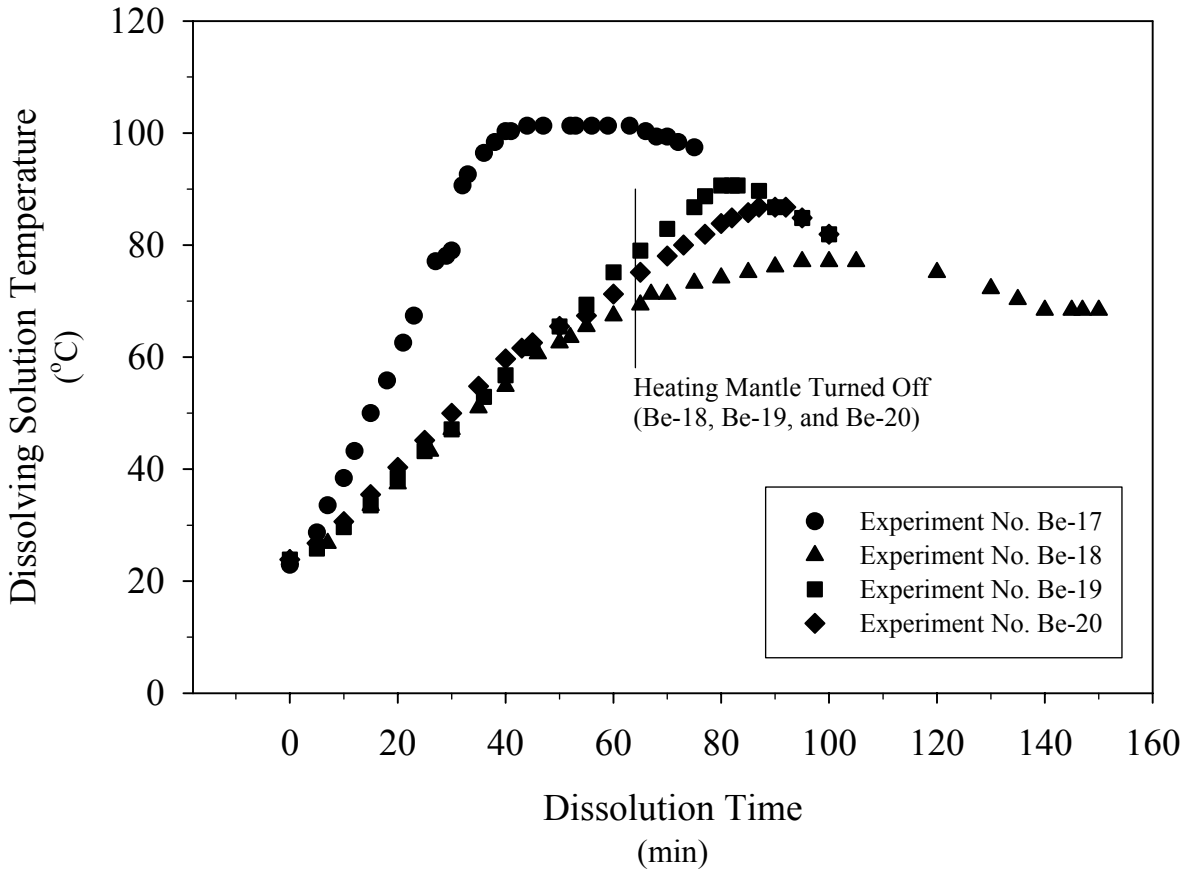

This page was intentionally left blank.

Appendix A Dissolution Rate Calculation for Be Metal Foils

The experimental data used to calculate the dissolution rate of the Be metal foils are presented in the following tables. The data include the mass, length, width, and thickness of the Be metal foils as functions of the cumulative dissolution time. Calculations presented in the tables include the surface area and mass to surface area ratios also as functions of the cumulative dissolution time.

Table A.1 Data for Experiment Be-1

Cumulative Dissolution Time (min)	Be Metal Foil Mass (g)	Be Metal Foil Length (mm)	Be Metal Foil Width (mm)	Be Metal Foil Thickness (mm)	Surface Area (cm^2)	Mass to Surface Area Ratio mg/cm^2
0.0	0.5909	25.01	25.12	0.53	13.10	45.12
1.0	0.5861	25.01	25.07	0.51	13.05	44.91
3.0	0.5722	24.91	24.04	0.51	12.48	45.86
7.0	0.5475	24.80	25.04	0.48	12.90	42.45
12.0	0.5163	24.89	24.98	0.46	12.89	40.04
22.0	0.4522	24.88	24.98	0.40	12.83	35.25
32.0	0.3876	24.77	24.84	0.33	12.63	30.68

Table A.2 Data for Experiment Be-2

Cumulative Dissolution Time (min)	Be Metal Foil Mass (g)	Be Metal Foil Length (mm)	Be Metal Foil Width (mm)	Be Metal Foil Thickness (mm)	Surface Area (cm^2)	Mass to Surface Area Ratio mg/cm^2
0.0	0.3874	24.80	24.95	0.33	12.70	30.50
5.0	0.3555	24.66	24.90	0.30	12.58	28.26
10.0	0.3229	24.75	24.84	0.27	12.56	25.70
15.0	0.2874	24.75	24.77	0.26	12.52	22.96
20.0	0.2527	24.63	24.72	0.24	12.41	20.36
25.0	0.2189	24.66	24.67	0.19	12.35	17.72
30.0	0.1849	24.53	24.61	0.16	12.23	15.12

Table A.3 Data for Experiment Be-3

Cumulative Dissolution Time (min)	Be Metal Foil Mass (g)	Be Metal Foil Length (mm)	Be Metal Foil Width (mm)	Be Metal Foil Thickness (mm)	Surface Area (cm^2)	Mass to Surface Area Ratio mg/cm^2
0.0	0.5909	24.97	25.06	0.51	13.03	45.37
5.0	0.5534	25.00	25.06	0.49	13.02	42.50
10.0	0.5109	24.93	24.95	0.45	12.89	39.64
15.0	0.4641	24.88	24.89	0.41	12.79	36.28
20.0	0.4134	24.85	24.87	0.37	12.73	32.48
25.0	0.3651	24.79	24.82	0.34	12.64	28.88
30.0	0.3200	24.75	24.75	0.29	12.54	25.52

Table A.4 Experiment No. Be-4

Cumulative Dissolution Time (min)	Be Metal Foil Mass (g)	Be Metal Foil Length (mm)	Be Metal Foil Width (mm)	Be Metal Foil Thickness (mm)	Surface Area (cm^2)	Mass to Surface Area Ratio mg/cm^2
0.0	0.3199	24.71	24.83	0.27	12.54	25.51
5.0	0.2415	24.63	24.64	0.23	12.36	19.53
10.0	0.1680	24.54	24.57	0.17	12.23	13.74
15.0	0.1047	24.58	24.62	0.11	12.21	8.57
20.0	0.0479	24.58	24.62	0.03	12.13	3.95
22.0	0.0258	24.58	24.62	0.04	12.14	2.12

Table A.5 Data for Experiment Be-5

Cumulative Dissolution Time (min)	Be Metal Foil Mass (g)	Be Metal Foil Length (mm)	Be Metal Foil Width (mm)	Be Metal Foil Thickness (mm)	Surface Area (cm^2)	Mass to Surface Area Ratio mg/cm^2
0.0	0.5898	25.00	25.14	0.52	13.09	45.05
5.0	0.3720	24.82	24.82	0.47	12.79	29.09
10.0	0.2026	24.56	24.58	0.2	12.27	16.51
13.0	0.1273	24.53	24.60	0.14	12.21	10.43
16.0	0.0551	24.53	24.60	0.07	12.14	4.54

Table A.6 Data for Experiment Be-6

Cumulative Dissolution Time (min)	Be Metal Foil Mass (g)	Be Metal Foil Length (mm)	Be Metal Foil Width (mm)	Be Metal Foil Thickness (mm)	Surface Area (cm^2)	Mass to Surface Area Ratio mg/cm^2
0.0	0.5919	24.95	25.06	0.5	13.01	45.51
1.0	0.4806	24.89	24.93	0.45	12.86	37.38
4.0	0.1724	24.61	24.68	0.23	12.37	13.93
5.0	0.0870	24.61	24.68	0.13	12.28	7.09

Table A.7 Data for Experiment Be-7

Cumulative Dissolution Time (min)	Be Metal Foil Mass (g)	Be Metal Foil Length (mm)	Be Metal Foil Width (mm)	Be Metal Foil Thickness (mm)	Surface Area (cm^2)	Mass to Surface Area Ratio mg/cm^2
0.0	0.5939	25.10	25.10	0.55	13.15	45.16
5.0	0.5668	25.04	25.08	0.51	13.07	43.36
10.0	0.5348	24.94	25.00	0.46	12.93	41.36
15.0	0.5029	24.87	24.97	0.43	12.85	39.14
20.0	0.4720	24.78	24.83	0.42	12.72	37.10
25.0	0.4431	24.79	24.83	0.38	12.69	34.92
30.0	0.4179	24.74	24.84	0.38	12.67	32.99

Table A.8 Data for Experiment Be-8

Cumulative Dissolution Time (min)	Be Metal Foil Mass (g)	Be Metal Foil Length (mm)	Be Metal Foil Width (mm)	Be Metal Foil Thickness (mm)	Surface Area (cm^2)	Mass to Surface Area Ratio mg/cm^2
0.0	0.4177	24.81	24.82	0.33	12.64	33.04
5.0	0.3728	24.73	24.75	0.31	12.55	29.71
10.0	0.3260	24.66	24.73	0.28	12.47	26.14
15.0	0.2773	24.62	24.65	0.25	12.38	22.39
20.0	0.2302	24.54	24.64	0.21	12.30	18.72
25.0	0.1873	24.63	24.70	0.17	12.33	15.18
30.0	0.1464	24.46	24.64	0.14	12.19	12.01

Table A.9 Data for Experiment Be-9

Cumulative Dissolution Time (min)	Be Metal Foil Mass (g)	Be Metal Foil Length (mm)	Be Metal Foil Width (mm)	Be Metal Foil Thickness (mm)	Surface Area (cm^2)	Mass to Surface Area Ratio mg/cm^2
0.0	0.5920	25.05	25.11	0.53	13.11	45.15
1.0	0.4557	24.92	24.95	0.42	12.85	35.45
2.0	0.3269	24.79	24.81	0.26	12.56	26.03
3.0	0.2077	24.68	24.74	0.18	12.39	16.76
4.0	0.0998	23.85	24.65	0.11	11.86	8.41
5.0	0.0116	21.20	14.40	0.01	6.11	1.90

Table A.10 Data for Experiment Be-12

Cumulative Dissolution Time (min)	Be Metal Foil Mass (g)	Be Metal Foil Length (mm)	Be Metal Foil Width (mm)	Be Metal Foil Thickness (mm)	Surface Area (cm^2)	Mass to Surface Area Ratio mg/cm^2
0.0	0.1462	24.45	24.60	0.11	12.14	12.05
5.0	0.1321	24.56	24.59	0.09	12.17	10.86
10.0	0.1178	24.45	24.56	0.07	12.08	9.75
20.0	0.0902	24.48	24.54	0.09	12.10	7.45
30.0	0.0663	24.34	24.44	0.06	11.96	5.55
35.0	0.0521	24.31	24.47	0.05	11.95	4.36
40.0	0.0416	24.17	24.17	0.04	11.72	3.55
45.0	0.0297	23.75	23.87	0.03	11.37	2.61
50.0	0.0187	23.38	23.43	0.03	10.98	1.70

The mass to surface area ratio for each Be metal dissolution is plotted as a function of the cumulative dissolution time on the following figures. Linear regressions were performed for each data set; regression lines are shown on the figures. The slope of the regression line through the data is the Be metal dissolution rate in units of mg/cm^2-min.

Figure A.1 Dissolution Rate Calculation for Experiment Be-1

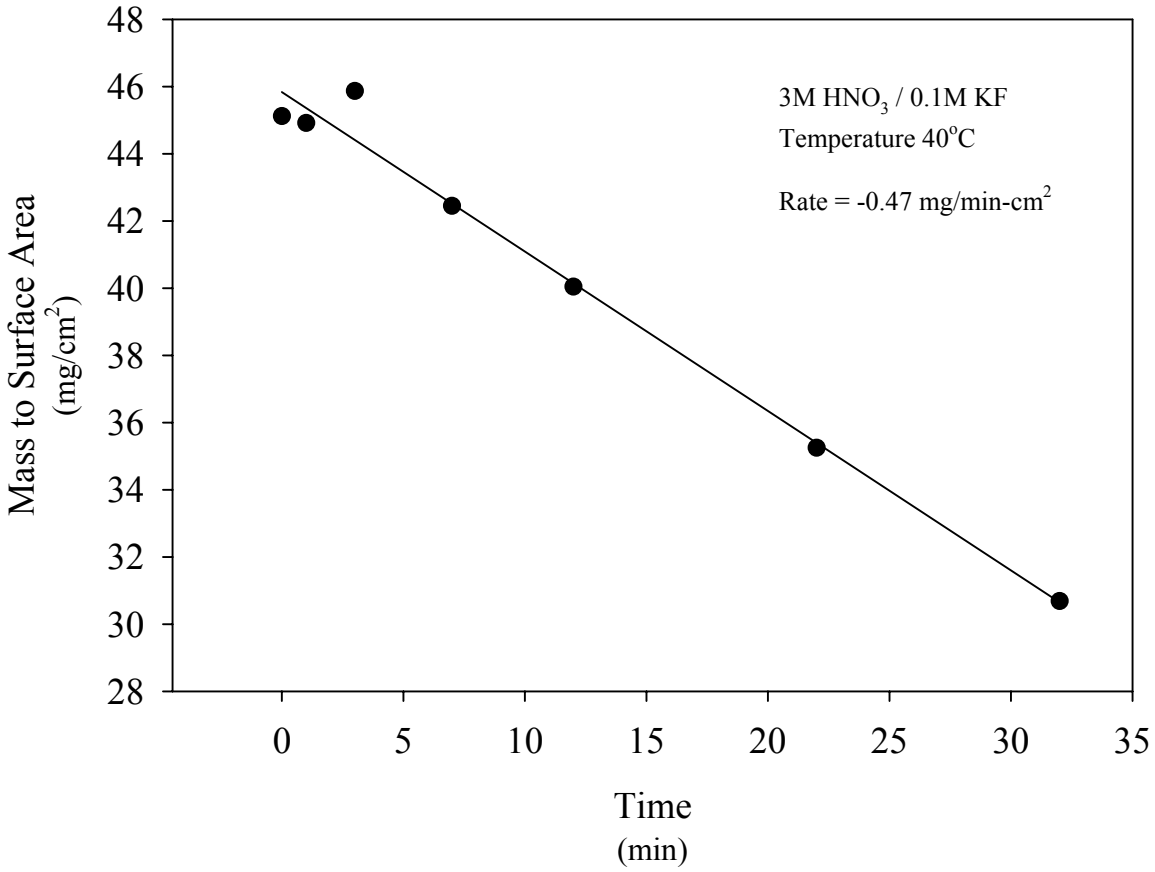

Figure A.2 Dissolution Rate Calculation for Experiment Be-2

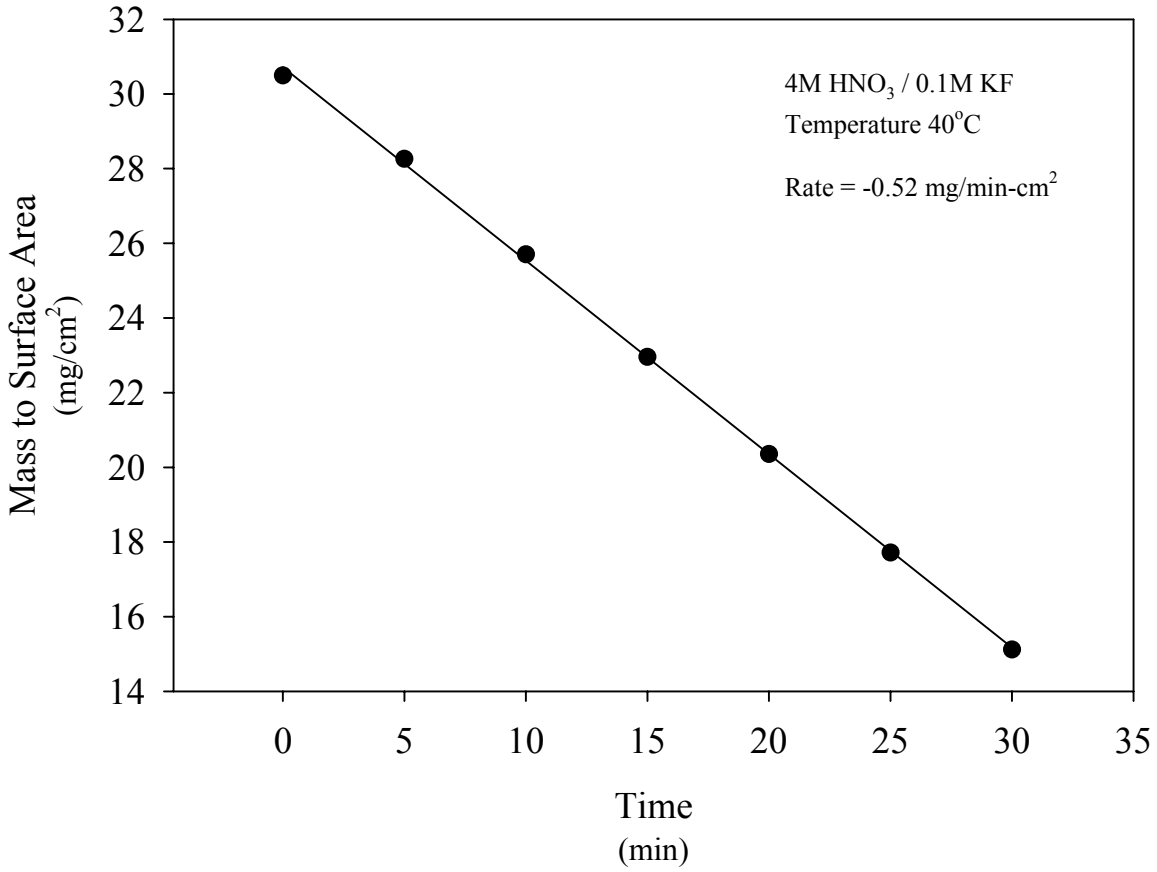

Figure A.3 Dissolution Rate Calculation for Experiment Be-3

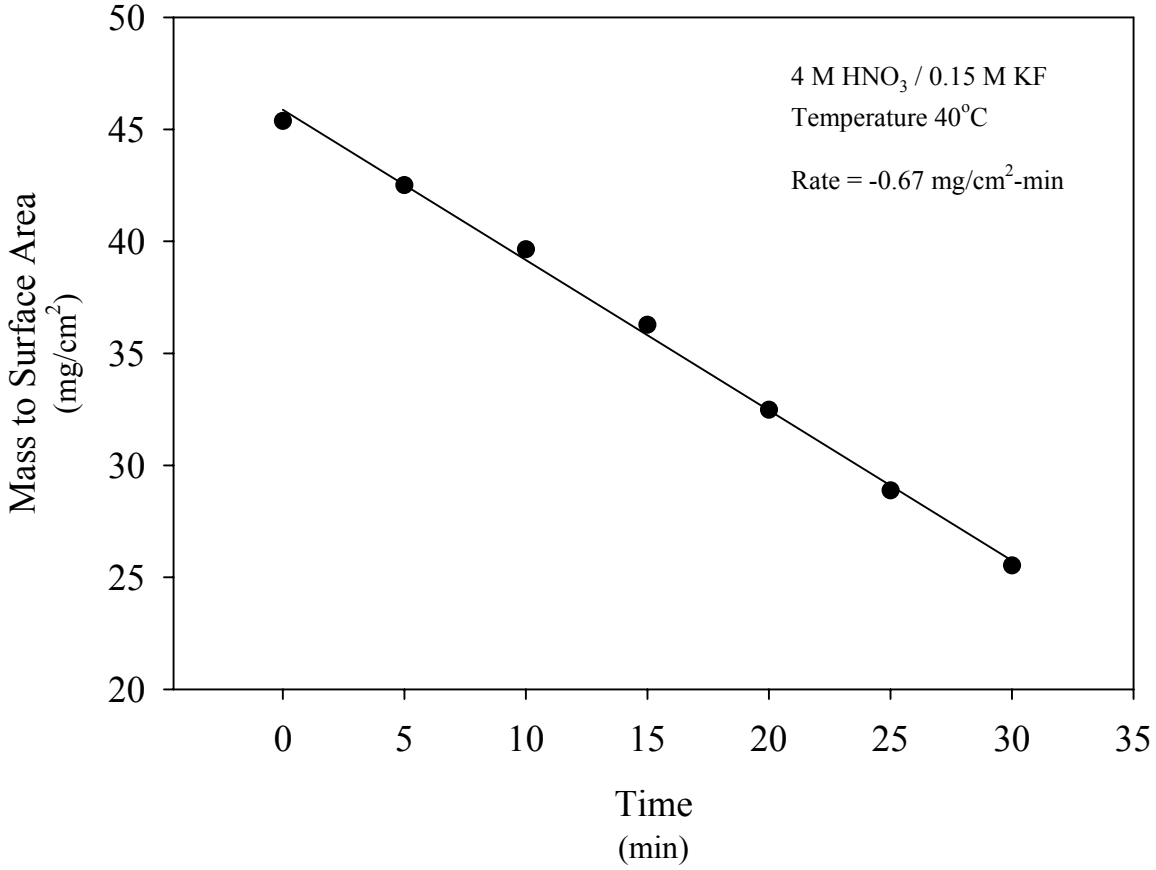

Figure A.4 Dissolution Rate Calculation for Experiment Be-4

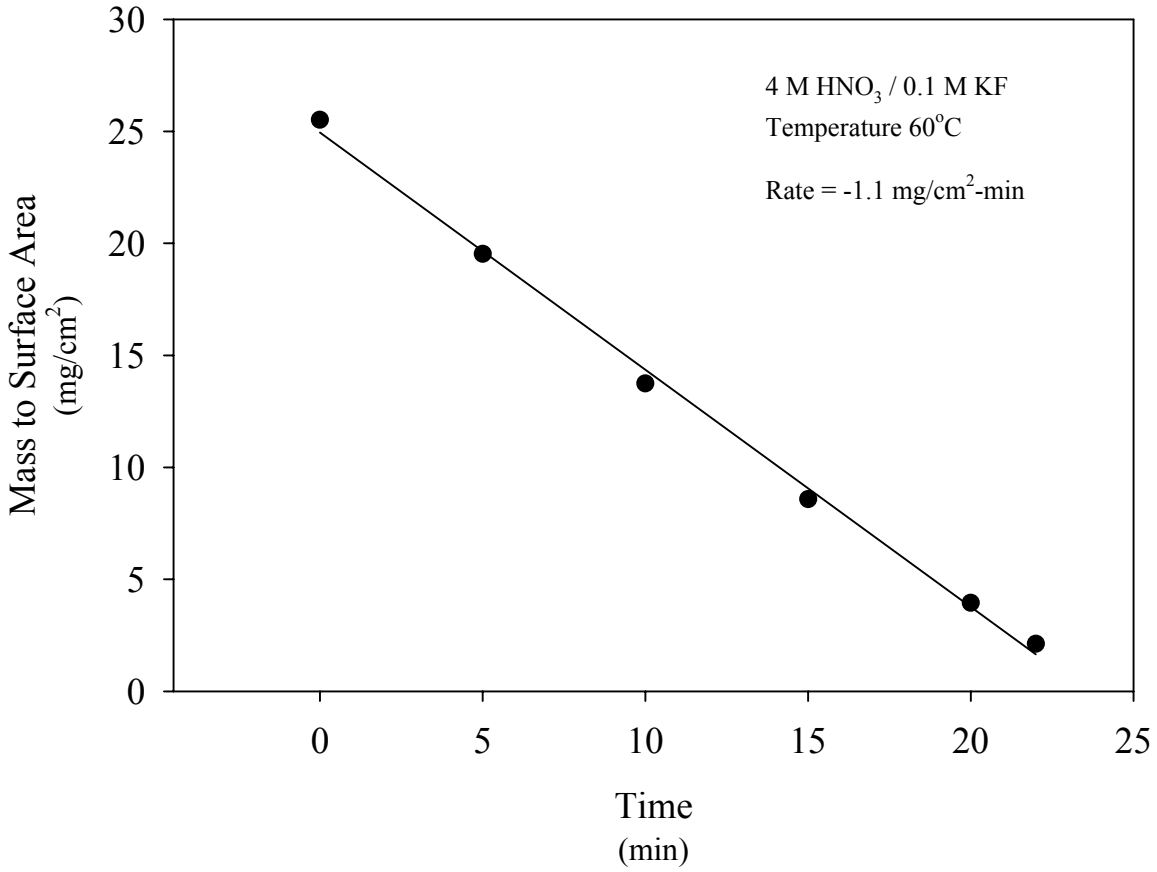

Figure A.5 Dissolution Rate Calculation for Experiment Be-5

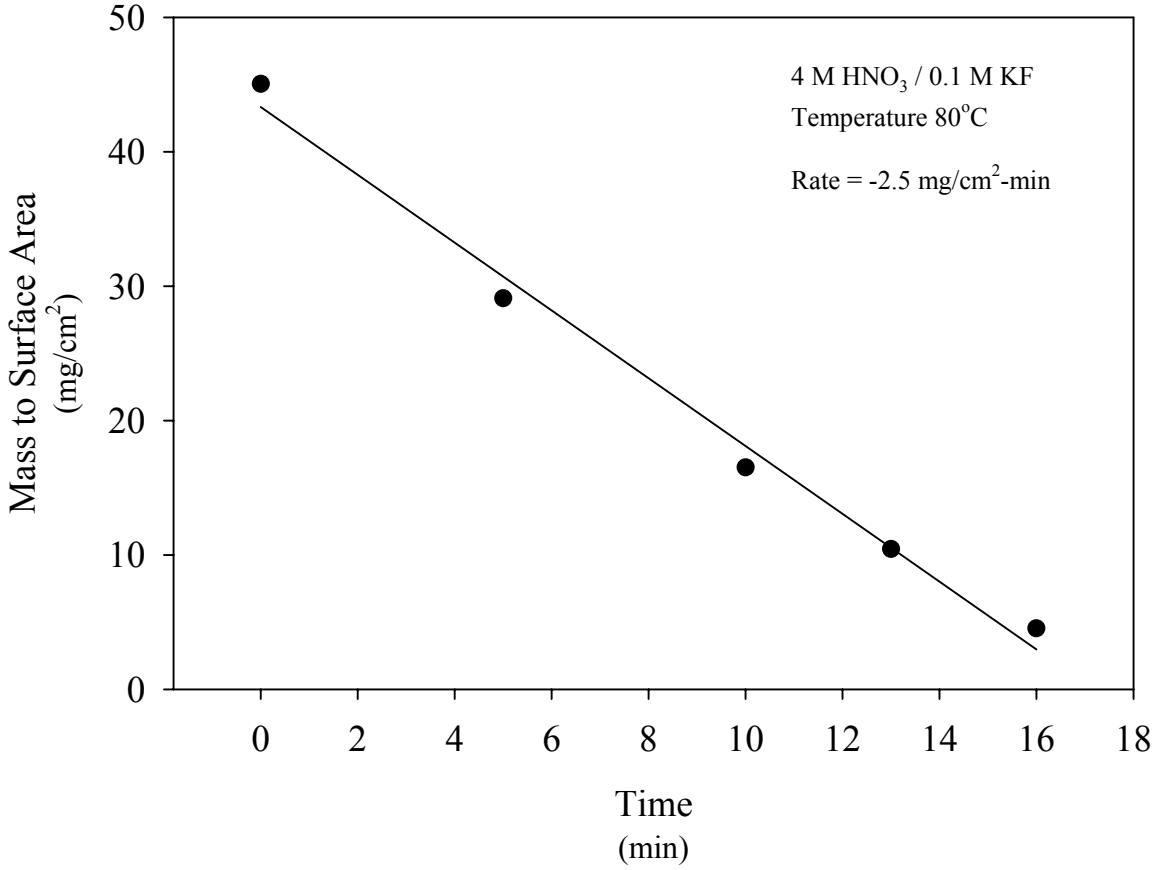

Figure A.6 Dissolution Rate Calculation for Experiment Be-6

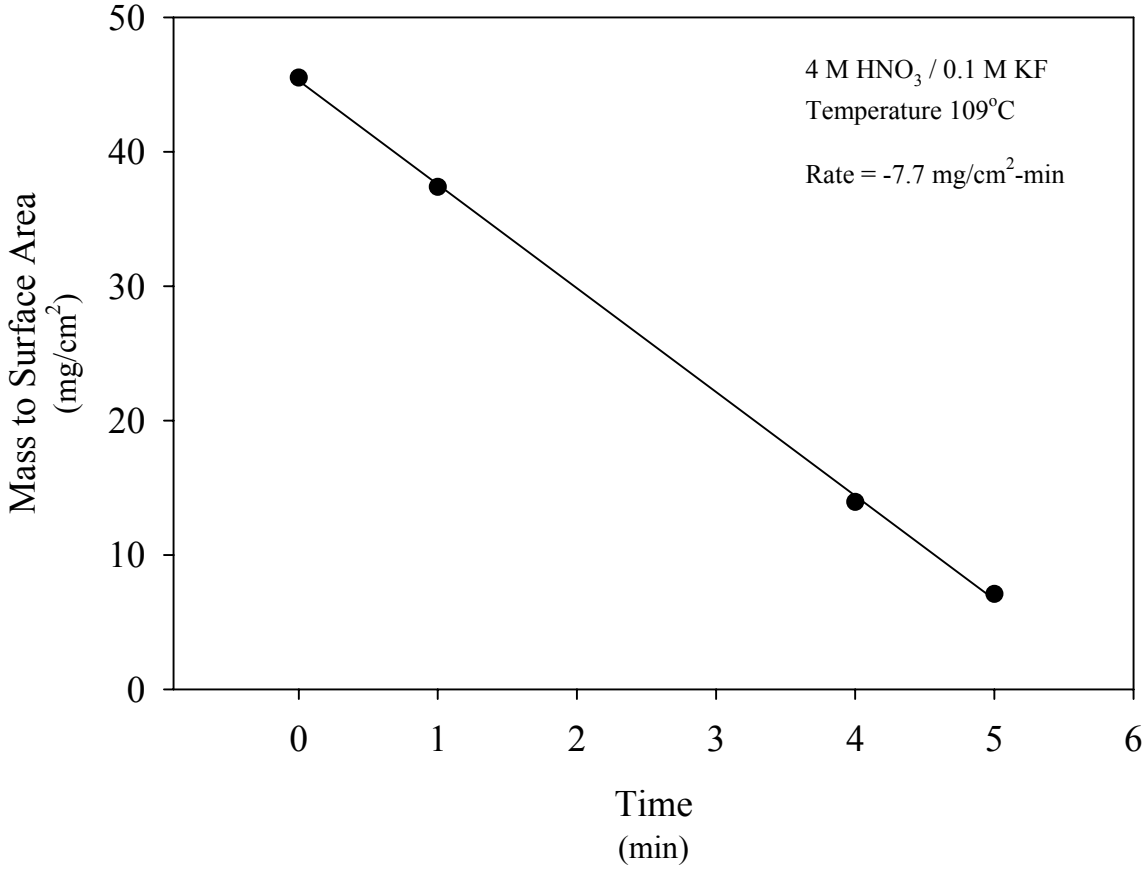

Figure A.7 Dissolution Rate Calculation for Experiment Be-7

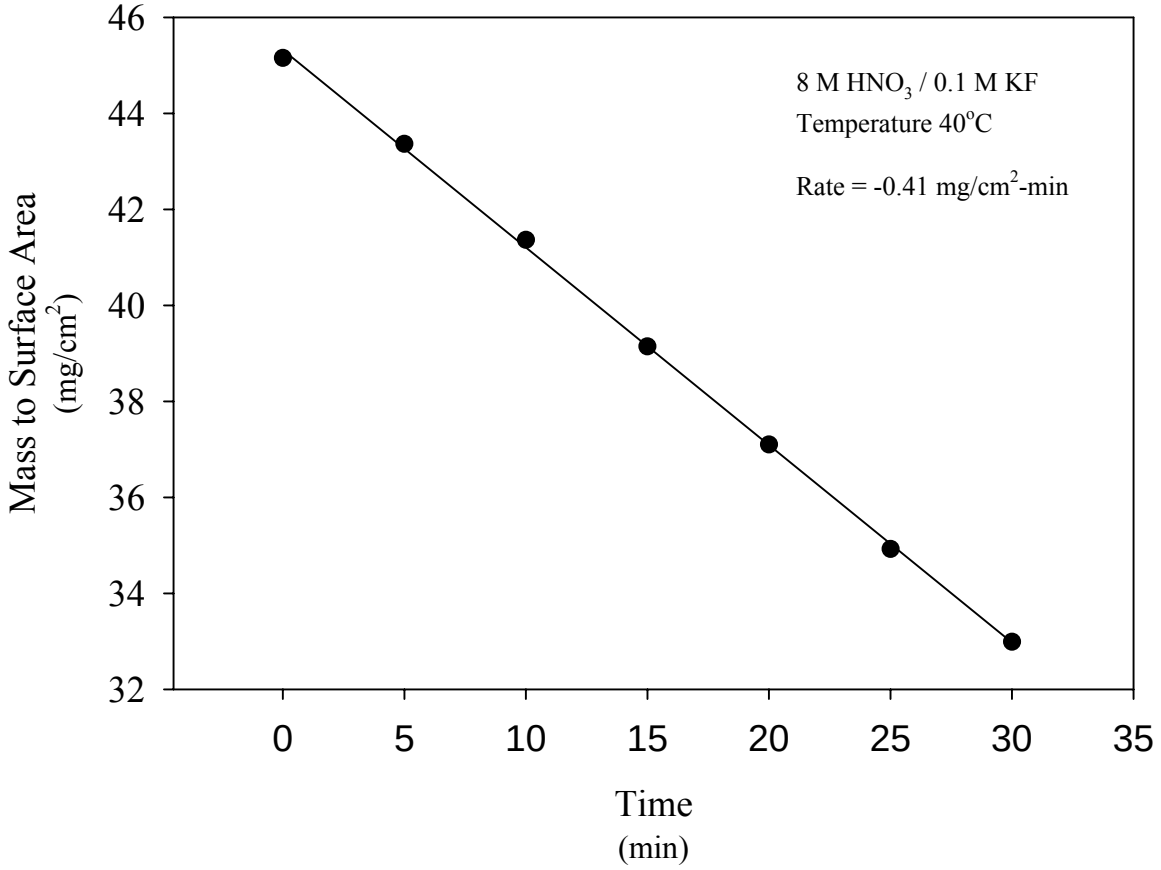

Figure A.8 Dissolution Rate Calculation for Experiment Be-8

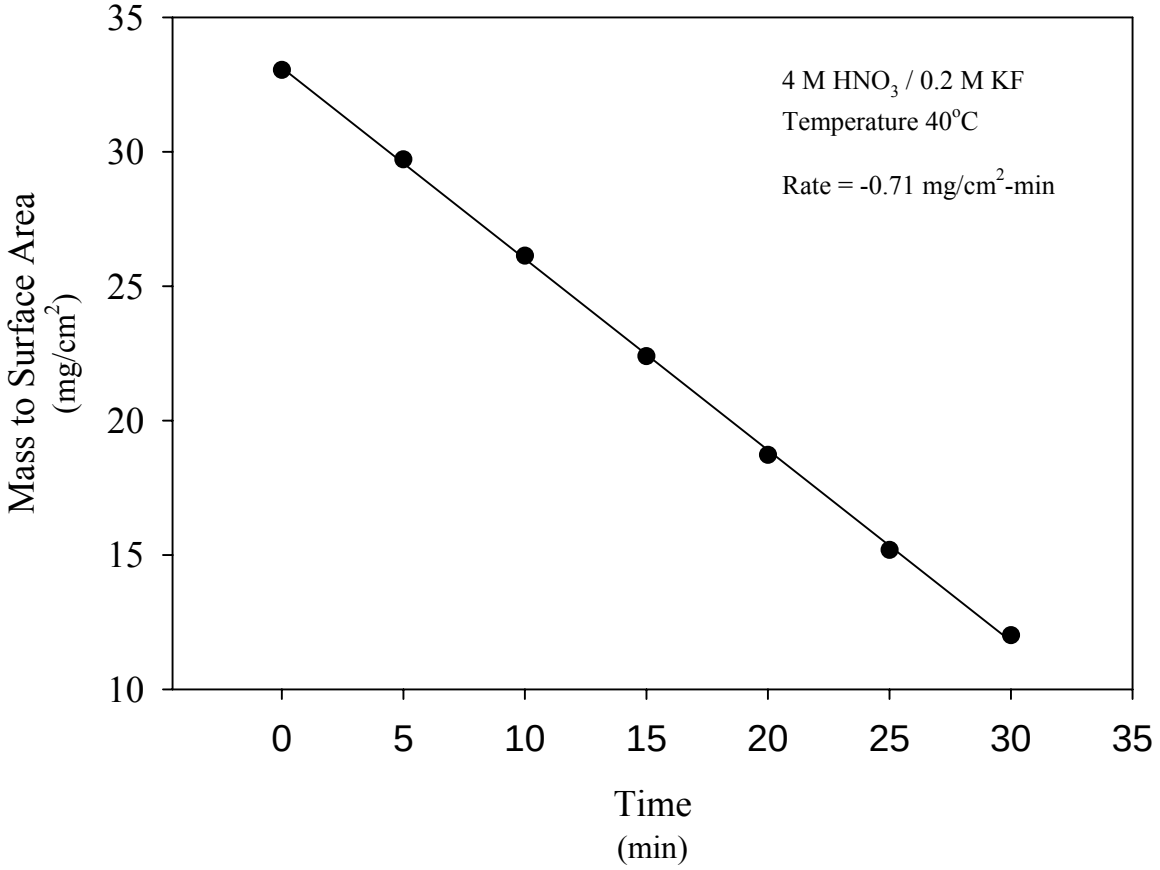

Figure A.9 Dissolution Rate Calculation for Experiment Be-9

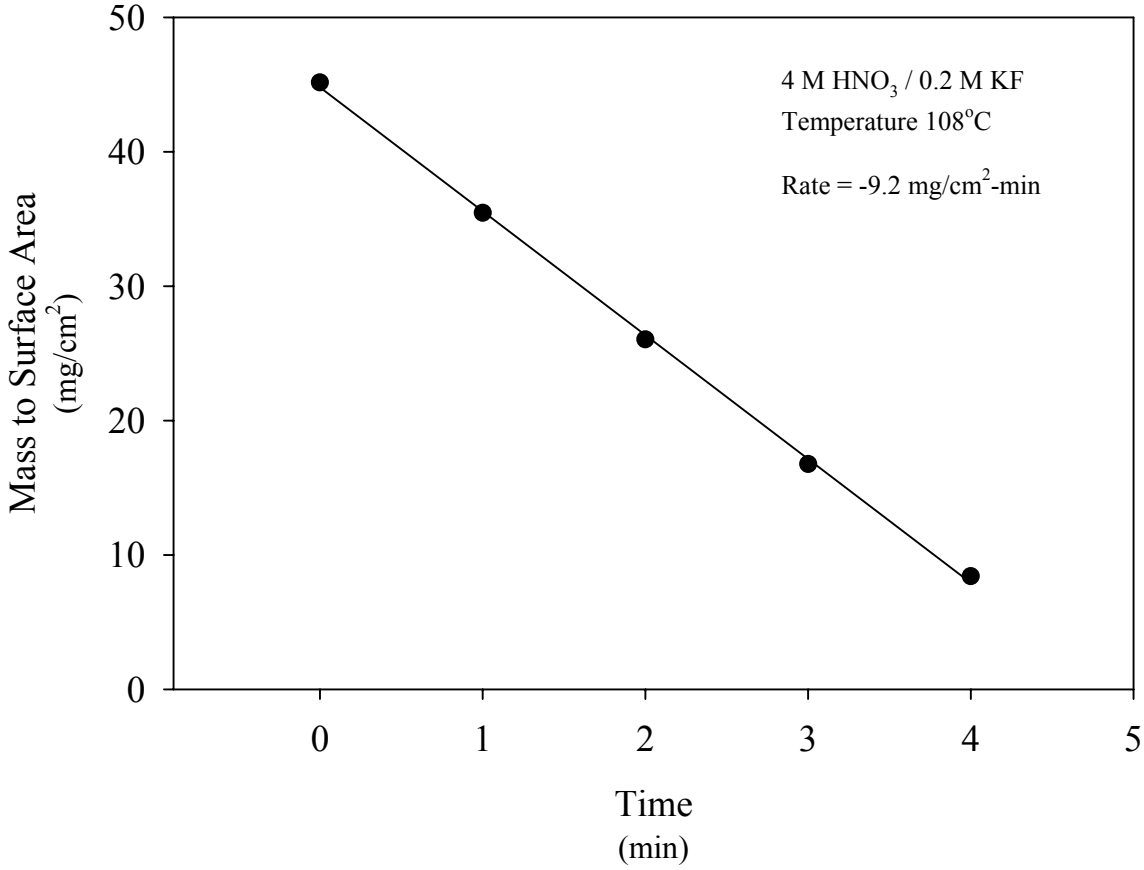

Figure A.10 Dissolution Rate Calculation for Experiment Be-12

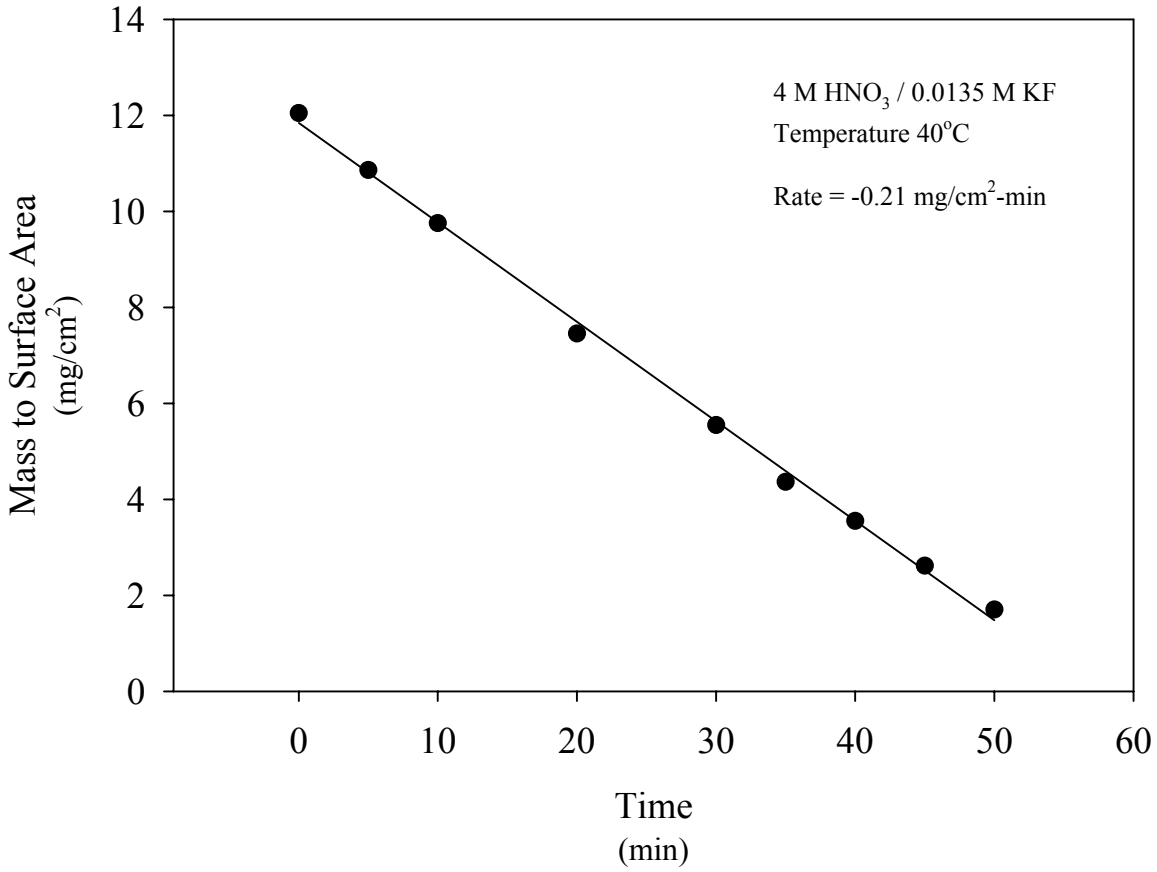

Appendix B Calculation of Adjusted Offgas Composition

The analyzed composition of the offgas measured during Be and Pu metal dissolutions must be corrected to account for dilution from gas in the dissolution vessel, condenser, plastic tubing, and sample bulb. To calculate the adjusted concentrations, ideal mixing of the gases in the void space is assumed and the effect of temperature variations in the gas is assumed negligible. For H_2 or any other component of the offgas, the adjusted concentration is calculated by material balance,

$$C_{gen}V_{gen} = C_{measured}\left(V_{void} + V_{bulb} + V_{gen}\right) - C_{initial}V_{void} \qquad (B.1)$$

where: C_{gen} = concentration of an offgas component in the generated gas (vol%)
$C_{measured}$ = concentration of an offgas component measured in a gas sample (vol%)
$C_{initial}$ = concentration of an offgas component before the sample collection (vol%)
V_{gen} = volume of gas collected in the Tedlar collection bag (mL)
V_{void} = void volume of dissolution vessel, condenser, and plastic tubing (mL)
V_{bulb} = volume of the gas sample bulb (mL).

Be Metal Foil Dissolutions

The Be metal foil dissolutions were performed in a 500 mL round bottom flask with a capacity of 700 mL. The capacity was measured by filling the flask with water. Each dissolution was performed using 300 mL of solution; therefore, the void volume of the flask was 400 mL. The void volume of the condenser and plastic tubing used to connect the sample bulb and Tedlar gas collection bag to the dissolution vessel were 34 and 40 mL, respectively. The volume of the condenser was measured by filling with water and the volume of the tubing was calculated from the length and inside diameter. The total void volume of the dissolution system was 474 mL. The volume of the gas sample bulbs was nominally 25 mL.

The analyzed and adjusted concentrations of each component and the volume of offgas generated during the three Be metal foil dissolutions are given in Table B.1. The adjusted concentrations were calculated using equation B.1. Since the offgas generated during the three dissolutions was collected in a single Tedlar bag and only one sample was taken, the concentration of all offgas components before sample collection ($C_{initial}$) is zero.

Table B.1 Offgas Characterization for Be Metal Foil Dissolutions

Exp. No.	Gas Volume (mL)	Analyzed Concentrations H_2 (vol%)	NO (vol%)	N_2O (vol%)	Adjusted Concentrations H_2 (vol%)	NO (vol%)	N_2O (vol%)
Be-13	511	21	14	2.6	42	28	5.1
Be-14	520	13	23	10	25	45	20
Be-15	508	23	14	2.1	46	28	4.2

Contaminated Be Dissolution

The contaminated Be metal dissolutions were performed in a 1000 mL round bottom flask with a capacity of 1188 mL. The capacity was measured by filling the flask with water. The dissolutions were performed using 650 mL of solution; therefore, the void volume of the flask was 538 mL. The void volume of the condenser and plastic tubing used to connect the sample bulb and Tedlar gas collection bag to the dissolution vessel were 34 and 6 mL, respectively. The volume of the condenser was measured by filling with water and the volume of the tubing was calculated from the length and inside diameter. The total void volume of the dissolution system was 578 mL. The volume of the gas sample bulbs was nominally 25 mL.

Experiment No. Be-17

The analyzed and adjusted concentrations and the volume of offgas generated during each sample period for experiment Be-17 are given in Table B.2. The adjusted concentrations were calculated using equation B.1. Since the dissolution system contained no H_2 or N_2O prior to the first sample, $C_{initial}$ is zero; however, in the subsequent samples, $C_{initial}$ is equal to the concentration measured in the previous gas sample ($C_{measured}$).

Table B.2 Offgas Characterization for Experiment No. Be-17

Sample No.	Gas Volume (mL)	Analyzed Concentration H_2 (vol%)	Analyzed Concentration N_2O (vol%)	Adjusted Concentration H_2 (vol%)	Adjusted Concentration N_2O (vol%)
1	233	8.7	<0.1	31	BDL
2	259	4.6	0.82	NR	2.7
3	608	3.8	0.36	3.2	NR
4	737	7.0	0.41	9.7	0.46
5	18	7.0	0.69	17	10.6

NR – not reported
BDL – below detection limit

The adjusted H_2 concentration for sample 2 and the adjusted N_2O concentration for sample 3 were not reported. The sharp decrease in the measured concentrations compared to the previous samples and the volume of offgas generated during the sample interval resulted in the calculation of inconsistent (negative) concentrations when the material balance was performed to calculate the adjusted concentrations. Therefore, it was assumed that the measured values were biased low.

Experiment Be-18

The analyzed and adjusted offgas concentrations and the volume of offgas generated during each sample period for experiment Be-18 are given in Table B.3. The adjusted concentrations were calculated used the same method as described for experiment Be-17.

Table B.3 Offgas Characterization for Experiment No. Be-18

Sample No.	Gas Volume (mL)	Analyzed Concentration H_2 (vol%)	Analyzed Concentration N_2O (vol%)	Adjusted Concentration H_2 (vol%)	Adjusted Concentration N_2O (vol%)
1	411	31	0.14	76	0.35
2	31	10	<0.1	NR	BDL

NR – not reported
BDL – below detection limit

The decrease in the measured H_2 concentration for sample 2 compared to sample 1 and the relatively small amount of offgas generated during the sample 2 time interval resulted in the calculation of an inconsistent (negative) adjusted concentration. Therefore, it was assumed that the measured value for sample 2 was biased low.

Experiment Be-19

The analyzed and adjusted offgas concentrations and the volume of offgas generated during each sample period for experiment Be-19 are given in Table B.4. The adjusted concentrations were calculated used the same method as described for experiment Be-17.

Table B.4 Offgas Characterization for Experiment No. Be-19

Sample No.	Gas Volume (mL)	Analyzed Concentration H_2 (vol%)	Analyzed Concentration N_2O (vol%)	Adjusted Concentration H_2 (vol%)	Adjusted Concentration N_2O (vol%)
1	428	7.9	0.044	19	0.11
2	342	8.0	1.7	8.8	4.6
3	193	2.8	0.56	NR	NR
4	487	2.0	0.39	1.2	0.21

NR – not reported

The decrease in the measured offgas concentrations for sample 3 compared to sample 2 and the smaller amount of offgas generated during the sample 3 time interval resulted in the calculation of inconsistent (negative) adjusted concentrations. Therefore, it was assumed that the measured values for sample 3 were biased low.

Experiment Be-20

The analyzed and adjusted offgas concentrations and the volume of offgas generated during each sample period for experiment Be-20 are given in Table B.5. The adjusted concentrations were calculated used the same method as described for experiment Be-17.

Table B.5 Offgas Characterization for Experiment No. Be-20

Sample No.	Gas Volume (mL)	Analyzed Concentration H_2 (vol%)	Analyzed Concentration N_2O (vol%)	Adjusted Concentration H_2 (vol%)	Adjusted Concentration N_2O (vol%)
1	373	21	<0.1	55	BDL
2	265	12	0.51	NR	1.7
3	598	5.4	0.58	NR	0.67
4	504	4.6	0.91	3.9	1.3
5	213	3.6	0.41	1.3	NR

NR – not reported
BDL – below detection limit

Decreases in the measured concentrations of H_2 and N_2O from one sample to the next and relatively small amounts of collected offgas resulted in the calculation of inconsistent (negative) adjusted concentrations in several cases. Therefore, it was assumed that the measured values for these samples were biased low.

Pu Metal Dissolution

The mass dissolved, analyzed and adjusted offgas concentrations, and the volume of offgas generated during each sample period for the Pu metal dissolution are given in Table B.6. The adjusted concentrations were calculated using the same method as described for experiment Be-17.

Table B.6 Offgas Characterization for Pu Metal Dissolution Experiment

Sample No.	Pu Mass (g)	Offgas Volume (mL)	Analyzed Concentration H_2 (vol%)	Analyzed Concentration N_2O (vol%)	Adjusted Concentration H_2 (vol%)	Adjusted Concentration N_2O (vol%)
1	7.8130	132	0.47	0.25	2.6	1.4
2	5.0804	250	<0.1	<0.1	BDL	BDL

BDL – below detection limit

The concentrations of H_2 and N_2O in sample 2 were reported as being below the detection limit; however, concentrations of N_2 and oxygen reported for the sample were consistent with the ratio in air which is evidence that the sample was contaminated with air during the analysis.

Appendix C Analysis of Pu Metal and Residue Dissolving Solutions

The radiochemical analyses for the Pu metal dissolving solution are shown in Table C.1. The volume of the solution recovered following filtration was 664 mL.

Table C.1 Radiochemical Analysis of Pu Metal Dissolving Solution

Isotope	Activity (dpm/mL)	Concentration (g/L)	Mass (g)
^{238}Pu	1.54E+08	0.004	0.003
$^{239/240}$Pu	4.32E+09	27.03	17.95
^{241}Pu	8.97E+09	0.04	0.03
Total Pu			17.98
^{241}Am	3.27E+08	0.04	0.03

The concentrations of ^{238}Pu, ^{241}Pu, and ^{241}Am were calculated using the specific activity of each isotope. The concentration of $^{239/240}$Pu was calculated using a weighted average of the specific activities by assuming the ^{239}Pu to ^{240}Pu ratio was 94 to 6 % (i.e., weapons grade Pu). The mass of each isotope dissolved was then calculated using the volume of the recovered dissolving solution. The ICP-ES analysis for trace elements present in the solution is shown in Table C-2. The mass of each element in the table was also calculated using the volume of the recovered dissolving solution.

Table C.2 Elemental Analysis for Pu Metal Dissolving Solution

Element	Concentration (mg/L)	Mass (g)
Ag	15.0	0.01
Al	186	0.12
B	20.1	0.01
Ba	14.5	0.01
Be	0.426	0.00
Ca	5.76	0.00
Cd	3.88	0.00
Ce	310	0.21
Cr	3.49	0.00
Cu	68.7	0.05
Fe	14.7	0.01
Gd	20.9	0.01
K	3280	2.18
La	33.8	0.02
Li	5.64	0.00
Mg	12.2	0.01
Mn	16.1	0.01

Table C.2 Continued

Element	Concentration (mg/L)	Mass (g)
Mo	39.1	0.03
Na	<4.34	N/A
Ni	15.2	0.01
P	29.6	0.02
Pb	17.9	0.01
S	<4.44	N/A
Sb	36.0	0.02
Si	84.8	0.06
Sn	59.7	0.04
Sr	14.1	0.01
Ti	<0.140	N/A
U	206	0.14
V	2.63	0.00
Zn	2.69	0.00
Zr	7.24	0.00

N/A – Not Applicable

The radiochemical analyses for the solution used to dissolve the residue from the Pu metal dissolution are shown in Table C.3. The volume of the dissolving solution recovered following filtration was 239 mL.

Table C.3 Radiochemical Analysis of Residue Dissolving Solution

Isotope	Activity (dpm/mL)	Concentration (g/L)	Mass (g)
^{238}Pu	4.77E+07	0.001	0.0003
$^{239/240}$Pu	1.26E+09	7.88	1.88
^{241}Pu	2.78E+09	0.01	0.00
Total Pu			1.89
^{241}Am	6.23E+07	0.01	0.002

The concentrations and masses of each isotope were calculated in the same manner as used for the data given in Table C.1. The ICP-ES analysis for trace elements present in the dissolving solution is shown in Table C.4. The mass of each element was calculated using the volume of the recovered solution.

Table C.4 Elemental Analysis for Residue Dissolving Solution

Element	Concentration (mg/L)	Mass (g)
Ag	5.29	0.00
Al	84.2	0.02
B	20.2	0.00
Ba	4.93	0.00
Ca	4.06	0.00
Cd	1.18	0.00
Ce	127	0.03
Cr	2.22	0.00
Cu	25.0	0.01
Fe	16.0	0.00
Gd	7.78	0.00
K	3620	0.87
La	14.5	0.00
Li	1.55	0.00
Mg	6.17	0.00
Mn	5.65	0.00
Mo	14.6	0.00
Na	21.5	0.01
Ni	7.16	0.00
P	<37.6	N/A
Pb	<26.5	N/A
S	<11.1	N/A
Sb	13.4	0.00
Sn	32.9	0.01
Sr	5.51	0.00
Ti	1.24	0.00
U	36.2	0.01
V	<1.95	N/A
Zn	1.84	0.00
Zr	6.10	0.00

N/A – Not Applicable